Journal of Applied Analysis and Computation
Volume 16, Number 4, August 2026, 1884–1922
Website:http://www.jaac-online.com
DOI:10.11948/20250264

DYNAMICS OF A LESLIE-GOWER PREDATOR-PREY MODEL WITH SMITH GROWTH AND ALLEE EFFECT

Zhennan Hu[1], Zhong Li[1,†], Fengde Chen[1] and Mengxin He[2]

Abstract In this paper, considering constant environment and changing environment, we study the bifurcation and transient dynamics of a Leslie-Gower predator-prey model incorporating Smith growth and Allee effect. In a constant environment, we show that the origin is an attractor, and the system admits at most two positive equilibria: One is a saddle and the other can be a weak focus of order four. The unique equilibrium is a saddle-node or a cusp of codimension three. As system parameters vary, the system undergoes a sequence of bifurcations, including saddle-node bifurcations, degenerate Bogdanov-Takens bifurcations of codimension three, and a degenerate Hopf bifurcation of codimension four. In a changing environment, by comparing these transient dynamics with the bifurcation structure of the corresponding constant environment system. We show that the system has rich transient dynamics, such as tracking of unstable equilibria or limit cycles, delay or avoid extinction, and slow and fast regime shifts. We show that low Smith growth or Allee effect is conducive to the stable coexistence of species, while the high Smith growth or Allee effect can eventually lead to the extinction of species.

Keywords Leslie-Gower, Allee effect, Smith growth, bifurcation, changing environment.

MSC(2010) 34C23, 34D20, 34H10, 92D25.

1. Introduction

The classic predator-prey model is one of the research contents in theoretical ecology, providing a basic framework for analyzing the interactions among species and the changes in their dynamic behaviors. A common predator-prey model is the Leslie-Gower predator-prey model [20, 21] which can be as follows

$$\begin{cases} \dot{x} = rx\Big(1-\dfrac{x}{K}\Big) - qxy, \\ \dot{y} = sy\Big(1-\dfrac{y}{nx}\Big), \end{cases} \tag{1.1}$$

where $x(t)$ and $y(t)$ represent the densities of prey and predator at time t, respectively, the term $\frac{y}{nx}$ describes the Leslie-Gower formulation, and nx represents the effective carrying capacity of the predator population due to its reliance on prey availability. Korobeinikov [18] proved that the unique positive equilibrium of system (1.1) is globally asymptotically stable. Subsequent studies [5, 7, 12, 16, 29, 37] have extended Leslie-Gower predator-prey model by introducing various functional responses, resulting in richer dynamics and complex bifurcation phenomena.

[†]The corresponding author.
[1]School of Mathematics and Statistics, Fuzhou University, Fuzhou 350116, China
[2]School of Computer and Data Science, Minjiang University, Fuzhou, Fujian 350108, China
Email: 3464500248@qq.com(Z. Hu), lizhong04108@163.com(Z. Li), fdchen@fzu.edu.cn(F. Chen), hemx@mju.edu.cn(M. He)

Another ecologically important concept is the Allee effect, first systematically described by W. C. Allee [1]. It refers to the reduced fitness or growth rate of a population at low densities due to difficulties in mating, cooperative behaviors, or predator avoidance. Incorporating the Allee effect into predator-prey models reveals bistability and extinction thresholds that are critical for understanding species persistence. From an ecological perspective, the Allee effect emphasizes the vulnerability of populations at low densities. When population size falls below a critical threshold, reduced mating success, weakened cooperative behaviors, and increased predation risk can significantly impair population growth. As a consequence, populations subject to strong Allee effects may experience an extinction threshold, beyond which recovery becomes impossible even under favorable environmental conditions. In predator–prey systems, the Allee effect can therefore generate multiple stable states and fundamentally alter persistence and extinction outcomes, which is particularly relevant for conservation and population management. Gonzáles-Olivares et al. [30] introduced the Allee effect on prey into system (1.1), and proposed the following system

$$\begin{cases} \dot{x} = rx\Big(1 - \dfrac{x}{K}\Big)(x - m) - qxy, \\ \dot{y} = sy\Big(1 - \dfrac{y}{nx}\Big), \end{cases} \tag{1.2}$$

where m is the Allee threshold. System (1.2) exhibits more complex dynamics than the classical system (1.1), including bistability, Hopf bifurcation, and Bogdanov-Takens bifurcation. Moreover, Yin et al. [39] incorporated the effect of prey refuge on system (1.2). Using the prey refuge and Allee effect as threshold condition, the authors investigated the stability and bifurcation of system, and showed that system can undergo degenerate Bogdanov-Takens bifurcation of codimension three and degenerate Hopf bifurcation of codimension two. Many researchers have explored predator-prey model with Allee effect and various forms of functional responses [6, 15, 23, 32], while other studies have focused on different types of Allee effect [17, 22, 25, 40].

In many ecological scenarios, the logistic equation is $\dot{x} = rx(1 - \frac{x}{k})$, assuming that the average growth rate of a species $\frac{\dot{x}}{x}$ would decrease linearly with its population density, which is unrealistic for some species. For example, by experiment, Smith [34] revealed that the early-stage growth of Daphnia populations depends on both food availability and metabolic maintenance, whereas at higher densities, food is only sufficient for survival, not growth. Biologically, the Smith growth model provides a more realistic description of population growth under limited and saturating food resources. Unlike logistic growth, it captures the trade-off between energy intake and metabolic maintenance. At low population densities, sufficient resources promote population growth, whereas at higher densities, increased metabolic costs suppress reproduction before the carrying capacity is reached. This mechanism reflects empirical observations in natural populations and highlights the importance of food limitation and metabolic constraints in shaping population dynamics. Hence, Smith [34] addressed this limitation by proposing a nonmonotonic growth model, that is $\dot{x} = rx\frac{K-x}{K+ax}$, where a is a parameter reflecting the metabolic cost of maintaining the population. The Smith growth model, sometimes called the "limited food" model, accounts for resource limitation and saturation effects.

The predator-prey model with Smith growth has been studied in various situations: Pal et al. [31] investigated a predator-prey model incorporating the Smith growth function, prey refuge, and toxicant-induced predator mortality. They analyzed the stability of system and demonstrated the occurrence of Hopf bifurcation. Bai et al. [4] discussed a predator-prey model with a Smith growth function and the addition predation term, and investigated the stability and Hopf bifurcation of system, as well as the existence of a heteroclinic orbit loop and limit

cycles. Fu and Jiang [11] considered a diffusive predator-prey model with schooling behavior and Smith growth in prey, and discussed the existence of the Turing bifurcation and Hopf bifurcation. For more references about the Smith growth, see [10, 19, 24].

Motivated by the complementary roles of the Smith growth function and the Allee effect in shaping ecological dynamics, we propose the following Leslie-Gower predator-prey model with Smith growth and Allee effect

$$\begin{cases} \dot{x} = rx\Big(\dfrac{K-x}{K+ax}\Big)(x-m) - qxy, \\ \dot{y} = sy\Big(1-\dfrac{y}{nx}\Big), \end{cases} \tag{1.3}$$

where the coefficients all are positive, x and y stand for population densities of prey and predator at time t, respectively; r and s are the intrinsic growth rates of prey and predator, respectively; K is the carrying capacity of prey; q is the maximum rate of predation; m $(0 < m < K)$ is the strong Allee effect; a is the resource limitation; $\frac{r}{a}$ is the mass substitution rate of the population at K; and n is the quality of prey provided to the predator.

The study of populations responses to environmental fluctuations remains a central challenge in ecological research [2, 26]. In particular, linking transient dynamics under changing environments with the stable and unstable structures of corresponding constant environment systems can provide key insights into the mechanisms underlying regime shifts and population persistence. To describe the directional change in habitat quality, Arumugam et al. [3] proposed that the prey's carrying capacity is a linear function of time. Xiang et al. [38] considered the following Leslie-Gower predator-prey model with Holling II function response and generalist predator in a changing environment

$$\begin{cases} \dot{x} = rx\Big(1-\dfrac{x}{K}\Big) - \dfrac{qxy}{p+x}, \\ \dot{y} = sy\Big(1-\dfrac{y}{nx+e}\Big), \\ \dot{K} = \mu. \end{cases}$$

They demonstrated that environmental change can induce transient tracking of unstable states, leading to regime shifts whose timing depends critically on the rate of change. In a periodic environment, they found that the populations converge to a periodic solution or an invariant torus. Lu et al. [27] further showed that both the direction and speed of environmental change can delay or trigger extinction, especially in spatially structured ecosystems.

Inspired by [27, 38] and based on system (1.3), we introduce the following model in a changing environment:

$$\begin{cases} \dot{x} = rx\Big(\dfrac{K-x}{K+ax}\Big)(x-m) - qxy, \\ \dot{y} = sy\Big(1-\dfrac{y}{nx}\Big), \\ \dot{K} = \mu, \end{cases} \tag{1.4}$$

where μ denotes the rate of environmental change affecting the habitat's carrying capacity. From the third equation, the carrying capacity is modeled as $K(t) = K_0 + \mu t$ (K_0 is the initial value), where $\mu > 0\,(\mu < 0)$ represents linear environmental improvement (degradation).

In this paper, considering the constant environment, we discuss the stability and bifurcations of system (1.3), such as the degenerate Bogdanov-Takens bifurcation of codimension 3 and the

degenerate Hopf bifurcation of codimension 4. Considering the changing environment, based on the dynamics of system (1.3), we focus on the influence of the rate of environmental change μ on the dynamics of system (1.4). We also compare the resulting transient and long-term behaviors with the bifurcation structures of the corresponding constant environment system (1.3), aiming to predict possible regime shifts and assess population persistence.

The remaining paper is organized as follows. In Section 2, we study the equilibria and their types of system (1.3), and then discuss bifurcations, including saddle-node bifurcation, degenerate Bogdanov-Takens bifurcation of codimension 3 and degenerate Hopf bifurcation of codimension 4. In Section 3, we explore the impact of environmental change on the dynamics of system (1.4). Finally, we discuss our results in Section 4.

2. Constant environment

Under constant environment $\mu = 0$, we will give a complete analysis of the stability and high codimension bifurcations of system (1.3). For simplicity, using the following transformation

$$\bar{x} = \frac{x}{K}, \quad \bar{y} = \frac{y}{nK}, \quad \bar{t} = Krt,$$
$$\bar{q} = \frac{nq}{r}, \quad \bar{s} = \frac{s}{Kr}, \quad \bar{m} = \frac{m}{K},$$

and dropping the bars, system (1.3) becomes the following system

$$\begin{cases} \dot{x} = \dfrac{x(1-x)}{1+ax}(x-m) - qxy, \\ \dot{y} = sy\Big(1 - \dfrac{y}{x}\Big), \end{cases} \tag{2.1}$$

where a, q, s are positive and $0 < m < 1$. Obviously, the positive invariant and bounded region of the system is $\Omega = \{(x, y) \in \mathbb{R}^2 \mid 0 < x \leq 1, 0 \leq y \leq 1\}$.

2.1. Preliminaries

Notice that system (2.1) is not defined in $x = 0$. Therefore, using blow-up method, we will discuss the dynamics of system (2.1) near the origin.

Lemma 2.1. *The origin of system* (2.1) *is an attractor.*

Proof. Letting $dt = x(1 + ax)d\tau$, system (2.1) is topologically equivalent to the following system

$$\begin{cases} \dot{x} = x^2\Big[(1-x)(x-m) - qy(1+ax)\Big], \\ \dot{y} = sy(1+ax)(x-y), \end{cases} \tag{2.2}$$

and it is well defined in axis $x = 0$. Obviously, when $x = 0$, we have $\dot{x} = 0$ and $\dot{y} = -sy^2 < 0$, which means that system (2.2) has the invariant line $x = 0$. The Jacobian matrix of system (2.2) at $(0, 0)$ is

$$J(0,0) = \begin{pmatrix} 0 & 0 \\ 0 & 0 \end{pmatrix}.$$

Next, we use the blow-up method of Chapter 3.1 in [41] to prove the stability of the origin of system (2.2). Using the transformation $x = u, y = uv$, $u\mathrm{d}\tau = \mathrm{d}t$, system (2.2) becomes

$$\begin{cases} \dot{u} = -u(aqu^2v + quv - mu + u^2 + m - u), \\ \dot{v} = v(aqvu^2 - asuv + asu + quv - mu - sv + u^2 + m + s - u). \end{cases} \tag{2.3}$$

Therefore system (2.3) has two boundary equilibria $(0,0)$ and $(0, \dfrac{m+s}{s})$. The Jacobian matrix of system (2.3) at $(0,0)$ is

$$J(0,0) = \begin{pmatrix} -m & 0 \\ 0 & m+s \end{pmatrix}.$$

Obviously, $(0,0)$ is a saddle (see Figure 1(a)). The Jacobian matrix of system (2.3) at $(0, \dfrac{m+s}{s})$ is

$$J(0, \frac{m+s}{s}) = \begin{pmatrix} -m & 0 \\ -\dfrac{(m+s)(asm - qm + ms - qs + s)}{s^2} & -(m+s) \end{pmatrix},$$

which implies that $(0, \frac{m+s}{s})$ is an attractor (see Figure 1(a)). Combining the above results, the origin of system (2.1) is an attractor (see Figure 1(b)). The proof is completed. □

Remark 2.1. From Lemma 2.1, the origin $(0,0)$ of system (2.1) is an attractor. More precisely, when the predation rate q is sufficiently large ($q \geq \max_{x\in(0,1)} \frac{(1-x)(x-m)}{x(1+ax)}$), the origin $(0,0)$ is globally asymptotically stable. Indeed, under this condition, the system admits no positive interior equilibrium. Moreover, the feasible region is positively invariant and bounded. By the Poincaré–Bendixson theorem, the absence of interior equilibria and periodic orbits implies that every trajectory converges to the only remaining equilibrium, namely the origin $(0,0)$.

From a biological point of view, the global asymptotic stability of the origin corresponds to the extinction of both predator and prey populations. Excessively strong predation pressure prevents the prey population from persisting, while the predator population subsequently collapses due to the depletion of its food resource.

2.2. Existence and stability of equilibria

In this section, we discuss the equilibria of system (2.1) and investigate its existence and types.

Firstly, we discuss the existence and stability of the boundary equilibrium of system (2.1). It is easy to see that system (2.1) always has two boundary equilibria $E_K(1,0)$ and $E_m(m,0)$. By direct computation, the Jacobian matrix of system (2.1) evaluated at E_K and E_m reveals that each equilibrium possesses at least one positive eigenvalue. Therefore, both equilibria are unstable.

Next, we want to discuss the positive equilibrium of system (2.1). Let $\dot{x} = \dot{y} = 0$ in system (2.1), then

$$\begin{cases} \dfrac{(x-m)(1-x)}{1+ax} - qy = 0, \\ 1 - \dfrac{y}{x} = 0. \end{cases}$$

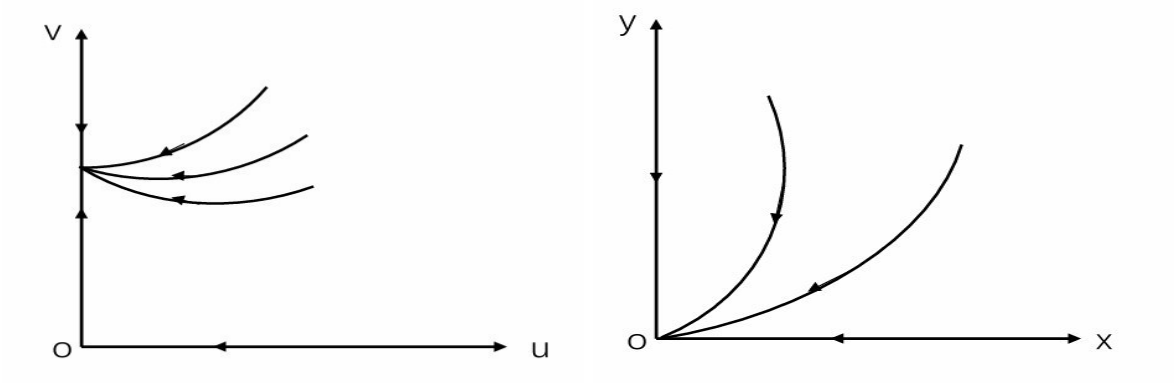

(a) (b)

Figure 1. (a) For system (2.3), $(0,0)$ is a saddle, $(0, \frac{m+s}{s})$ is an attractor. (b) The origin of system (2.1) is an attractor.

For the possible positive equilibrium, we just consider the following equation

$$\begin{cases} (aq+1)x^2 - (m+1-q)x + m = 0, \\ y = x. \end{cases}$$

Denote

$$F(x) = (aq+1)x^2 - (m+1-q)x + m, \tag{2.4}$$

where the derivative of (2.4) is

$$f(x) = 2(aq+1)x - (m+1-q).$$

Obviously, $m \le q-1$ implies that (2.4) has no positive root. Hence, in the following discussion, we only consider $\max\{q-1, 0\} < m < 1$.

The discriminant of (2.4) is

$$\Delta = 4mq(a^* - a),$$

where

$$a^* = \frac{m^2 - 2(q+1)m + (q-1)^2}{4mq}.$$

Obviously, when $q \ge 2$, equation (2.4) has no positive root. When $1 \le q < 2$ or $0 < q < 1$ with $(1-\sqrt{q})^2 \le m < 1$, we have $a^* \le 0$, which implies that equation (2.4) has no positive root.

Define

$$x_1 = \frac{m+1-q-\sqrt{\Delta}}{2(aq+1)}, \quad x_2 = \frac{m+1-q+\sqrt{\Delta}}{2(aq+1)}, \quad x_* = \frac{2m}{m-q+1},$$

and note that $x_1 < x_* < x_2$.

Consequently, when $0 < q < 1$ and $0 < m < (1-\sqrt{q})^2$, that is $a^* > 0$, equation (2.4) has no positive root if $a > a^*$, a unique positive root x_* if $a = a^*$, and two positive roots x_1, x_2 if $a < a^*$.

Next, we investigate that the existence of the positive roots of (2.4) in the interval $(m, 1)$. Note that

$$F(m) = aqm^2 + qm > 0,\ F(1) = aq + q > 0,$$
$$f(m) = 2amq + m + q - 1,\ f(1) = 2aq + q + 1 - m > 0.$$

When $0 < q < 1,\ 0 < m < (1 - \sqrt{q})^2$ and $0 < a \le a^*$, we have

$$f(m) \le 2a^*mq + m + q - 1 = \frac{(m - q + 1)(m - q - 1)}{2} < 0,$$

which means that $m < x_1 < x_* < x_2 < 1$. Therefore, we have the following result.

Lemma 2.2. *The existence of positive equilibria of system* (2.1) *are as follows:*
(i) if $0 < q < 1$, $0 < m < (1 - \sqrt{q})^2$ *and* $0 < a < a^*$, *system* (2.1) *has two distinct positive equilibria* $E_1(x_1, x_1)$ *and* $E_2(x_2, x_2)$*;*
(ii) if $0 < q < 1$, $0 < m < (1 - \sqrt{q})^2$ *and* $a = a^*$ *system* (2.1) *has a unique positive equilibrium* $E_*(x_*, x_*)$*;*
(iii) if $q \ge 1$*; or* $0 < q < 1,\ (1 - \sqrt{q})^2 \le m < 1$*; or* $0 < q < 1,\ 0 < m < (1 - \sqrt{q})^2,\ a > a^*$, *system* (2.1) *has no positive equilibrium.*

For any positive equilibrium $E(x, y)$, the Jacobian matrix of system (2.1) is

$$J_E = \begin{pmatrix} x\left(\dfrac{(1 - 2x + m)}{(1 + ax)} - \dfrac{a(1 - x)(x - m)}{(1 + ax)^2}\right) & -qx \\ s & -s \end{pmatrix},$$

and

$$Det(J_E) = \frac{s\left(a^2q\,x^3 + 2aq\,x^2 + a\,x^2 - am + qx - m + 2x - 1\right)}{(1 + ax)^2},$$
$$Tr(J_E) = \frac{1 - 2x + m}{1 + ax} - \frac{a(1 - x)(x - m)}{(1 + ax)^2} - s.$$

From $F(x) = 0$, we have

$$m = \frac{(aq + 1)x^2 + (q - 1)x}{x - 1}. \tag{2.5}$$

Substituting (2.5) into $Det(J_E)$ and $f(x)$, we get

$$Det(J_E) = \frac{xs}{1 + ax} f(x). \tag{2.6}$$

Obviously, from equation (2.6), we can know that $DetJ_{E_1} < 0$ and $DetJ_{E_2} > 0$, which implies that E_1 is a saddle. Then we have the following theorem.

Theorem 2.1. *Assume that the condition of Lemma 2.2* (*i*) *holds, then* E_1 *is always a saddle.*

Now we investigate the stability of E_2. By computation, we have

$$Tr(J_{E_2}) = s_* - s,$$

where

$$s_* = \frac{(1-2x_2+m)(ax_2+1)-(x_2-m)(1-x_2)a}{(ax_2+1)^2}.$$

Hence, if $s_* \le 0$, we obtain $Tr(J_{E_2}) < 0$, which implies that E_2 is stable. In the following discussion, we only consider $s_* > 0$. If $s_* > s > 0$, we can get $Tr(J_{E_2}) > 0$, which means that E_2 is unstable; if $s_* < s$, that is, $Tr(J_{E_2}) < 0$, E_2 is stable; if $s_* = s$, we have $Tr(J_{E_2}) = 0$, that is, E_2 is a weak focus with multiplicity at most four (see Theorem 2.6). Combining the above discussion, we can get the following theorem.

Theorem 2.2. *Assume that the condition of Lemma 2.2 (i) holds, then*
(1) if $s_* > s > 0$, E_2 is unstable;
(2) if $0 < s_* < s$ or $s_* \le 0$, E_2 is stable;
(3) if $s = s_* > 0$, E_2 is a weak focus with multiplicity at most four.

Now, we next discuss the dynamic behavior of the degenerate equilibrium $E_*(x_*, x_*)$. By calculation, when $0 < m < (1-\sqrt{q})^2$ and $0 < q < 1$, we have

$$Det(J_{E_*}) = 0,\ Tr(J_{E_*}) = s_1 - s,$$

where

$$s_1 = \frac{2qm}{m-q+1}.$$

Define

$$m_* = 2q - 3 + T,\ \ T = \sqrt{q^2-8q+8},$$

for $\frac{1}{3} < q < 4-2\sqrt{3}$.

Theorem 2.3. *Assume that $0 < m < (1-\sqrt{q})^2$ and $a = a^*$ hold.*
(1) When $0 < q < 1$, $s > s_1$ (or $0 < q < 1$, $0 < s < s_1$), E_* is a saddle-node, which includes a stable (or unstable) parabolic sector in the left.
(2) When $s = s_1$,
(2.1) E_* is a cusp of codimension two if $q \le \frac{1}{3}$; or $\frac{1}{3} < q < 4-2\sqrt{3}$ and $m \ne m_*$; or $4-2\sqrt{3} \le q < 1$;
(2.2) E_* is a cusp of codimension three if $\frac{1}{3} < q < 4-2\sqrt{3}$ and $m = m_*$.

Proof. (1) When $s \ne s_1$, that is $Det(J_{E_*}) = 0$, $Tr(J_{E_*}) \ne 0$, making the following transformation

$$\begin{aligned} &x = x_1 + x_*,\ \ y = y_1 + y_*;\\ &x_1 = -s_1(x_2 - y_2),\ \ y_1 = -s_1 x_2 + s y_2,\ \ \mathrm{d}t = (s_1 - s)d\tau, \end{aligned}$$

still denoting τ as t, system (2.1) becomes

$$\begin{cases} \dot{x}_2 = a_{20}x_2^2 + a_{11}x_2y_2 + a_{02}y_2 + o(|x_2, y_2|^2),\\ \dot{y}_2 = y_2 + b_{20}x_2^2 + b_{11}x_2y_2 + b_{02}y_2^2 + o(|x_2, y_2|^2), \end{cases}$$

where

$$a_{20} = -\frac{2sm\,q^2\,(m-q+1)}{(m-1-q)\,(m+q-1)\,(s_1-s)^2},$$

and a_{11}, a_{02}, b_{11}, b_{02}, b_{20} are expressed by s, x_*, q, which are omitted for brevity.

When $0 < m < (1-\sqrt{q})^2$, $0 < q < 1$ and $s \neq s_1$, we have $a_{20} < 0$. By Theorem 7.1 in Chapter 2 of [41], E_* is a saddle-node, which includes a stable (or unstable) parabolic sector in the left if $s > s_1$ (or $0 < s < s_1$), see Figures 2(a) and 2(b).

(2) When $s = s_1$, using the following transformations successively

$$x = x_1 + x_*, \quad y = y_1 + y_*;$$
$$x_1 = -s_1 x_2, \quad y_1 = -s_1 x_2 + y_2,$$

system (2.1) can be written as

$$\begin{cases} \dot{x}_2 = y_2 + \bar{a}_{20}x_2^2 + \bar{a}_{11}x_2y_2 + o(|x_2, y_2|^2), \\ \dot{y}_2 = \bar{b}_{20}x_2^2 + \bar{b}x_2y_2 + \bar{b}_{02}y_2^2 + o(|x_2, y_2|^2), \end{cases} \tag{2.7}$$

where

$$\bar{a}_{20} = \frac{2q^2m\,(m-q+1)}{(m-1-q)\,(m+q-1)}, \quad \bar{a}_{11} = -q,$$
$$\bar{b}_{20} = \frac{4q^3m^2}{(m+q-1)\,(m-1-q)}, \quad \bar{b}_{11} = -\frac{2q^2m}{m-q+1}, \quad \bar{b}_{02} = -\frac{s\,(m-q+1)}{2m}.$$

By Lemma 3.1 in [14], system (2.7) becomes

$$\begin{cases} \dot{X} = Y + o(|X, Y|^2), \\ \dot{Y} = DX^2 + EXY + o(|X, Y|^2), \end{cases}$$

where

$$D = \frac{4q^3m^2}{(m+q-1)\,(m-1-q)}, \quad E = \frac{2q^2m\left(m^2 + 2(3-2q)m + (3q-1)(q-1)\right)}{(m-q+1)\,(m+q-1)\,(m-1-q)}.$$

Notice that $0 < m < (1-\sqrt{q})^2$ and $0 < q < 1$. Then we obtain that $D \neq 0$. By simple calculation, if $q \leq \frac{1}{3}$; or $\frac{1}{3} < q < 4 - 2\sqrt{3}$ and $m \neq m_*$; or $4 - 2\sqrt{3} \leq q < 1$, we have $E \neq 0$, it implies that is E_* is a cusp of codimension two (see Figure 2(c)).

When $m = m_*$ and $\frac{1}{3} < q < 4 - 2\sqrt{3}$, we can get $E = 0$. Using the similar transformations in [38], we want to show that E_* is a cusp of codimension three. Making the following transformation,

$$x = x_1 + \frac{2m_*}{m_* - q + 1}, \quad y = y_1 + \frac{2m_*}{m_* - q + 1},$$

system (2.1) becomes

$$\begin{cases} \dot{x}_1 = \tilde{a}_{10}x_1 + \tilde{a}_{01}y_1 + \tilde{a}_{20}x_1^2 + \tilde{a}_{11}x_1y_1 + \tilde{a}_{30}x_1^3 + \tilde{a}_{40}x_1^4 + o(|x_1, y_1|^4), \\ \dot{y}_1 = \tilde{b}_{10}x_1 + \tilde{b}_{01}y_1 + \tilde{b}_{20}x_1^2 + \tilde{b}_{11}x_1y_1 + \tilde{b}_{02}y_1^2 + \tilde{b}_{30}x_1^3 + \tilde{b}_{21}x_1^2y_1 \\ \qquad + \tilde{b}_{12}x_1y_1^2 + \tilde{b}_{40}x_1^4 + \tilde{b}_{31}x_1^3y_1 + \tilde{b}_{22}x_1^2y_1^2 + o(|x_1, y_1|^4), \end{cases} \tag{2.8}$$

where the coefficients of system (2.8) are omitted for brevity.

Letting

$$\begin{aligned} x_2 &= x_1, \\ y_2 &= \tilde{a}_{10}x_1 + \tilde{a}_{01}y_1 + \tilde{a}_{20}x_1^2 + \tilde{a}_{11}x_1y_1 + \tilde{a}_{30}x_1^3 + \tilde{a}_{40}x_1^4 + o(|x_1, y_1|^4), \end{aligned}$$

system (2.8) becomes

$$\begin{cases} \dot{x}_2 = y_2, \\ \dot{y}_2 = \tilde{c}_{20}x_2^2 + \tilde{c}_{02}y_2^2 + \tilde{c}_{30}x_2^3 + \tilde{c}_{21}x_2^2y_2 + \tilde{c}_{12}x_2y_2^2 + \tilde{c}_{40}x_2^4 \\ \qquad +\tilde{c}_{31}x_2^3y_2 + \tilde{c}_{22}x_2^2y_2^2 + o(|x_2, y_2|^4), \end{cases} \tag{2.9}$$

where $\tilde{c}_{ij}$ can be represented by $\tilde{a}_{ij}$, $\tilde{b}_{ij}$, and their detailed expressions are omitted for brevity. In the following proof of this theorem, all the coefficients of systems are also omitted.

Next, making the following transformation,

$$x_3 = y_2,\ y_3 = (1 - \tilde{c}_{02}x_2)y_2,\ dt = (1 - \tilde{c}_{02}x_2)d\tau,$$

still rewriting τ as t, system (2.9) becomes

$$\begin{cases} \dot{x}_3 = y_3, \\ \dot{y}_3 = \tilde{d}_{20}x_3^2 + \tilde{d}_{30}x_3^3 + \tilde{d}_{21}x_3^2y_3 + \tilde{d}_{12}x_3y_3^2 + \tilde{d}_{40}x_3^4 \\ \qquad +\tilde{d}_{31}x_3^3y_3 + \tilde{d}_{22}x_3^2y_3^2 + o(|x_3, y_3|^4). \end{cases} \tag{2.10}$$

When $\frac{1}{3} < q < 4 - 2\sqrt{3}$,

$$\tilde{d}_{20} = \frac{q^2\,(2q - 3 + T)}{q - 2 + T} < 0.$$

Making a transformation as follows

$$x_4 = -x_3,\ y_4 = \frac{y_3}{\sqrt{-\tilde{d}_{20}}},\ \tau_1 = \sqrt{-\tilde{d}_{20}}t,$$

and still denoting τ_1 as t, system (2.10) becomes

$$\begin{cases} \dot{x}_4 = y_4, \\ \dot{y}_4 = x_4^2 + \tilde{e}_{30}x_4^3 + \tilde{e}_{21}x_4^2y_4 + \tilde{e}_{12}x_4y_4^2 + \tilde{e}_{40}x_4^4 + \tilde{e}_{31}x_4^3y_4 + \tilde{e}_{22}x_4^2y_4^2 + o(|x_4, y_4|^4). \end{cases} \tag{2.11}$$

By Lemma 2 in [13], system (2.12) is locally topologically equivalent to

$$\begin{cases} \dot{x}_5 = y_5, \\ \dot{y}_5 = x_5 + Gx_5^3y_5 + o(|x_5, y_5|^4), \end{cases} \tag{2.12}$$

where

$$G = -\frac{\sqrt{2}(q - 2 + T)^{\frac{3}{2}}G_1}{8\,(3q - 4 + T)^{\frac{5}{2}}\,(T + q - 4)^{\frac{5}{2}}\,(2q - 3 + T)^{\frac{5}{2}}},$$

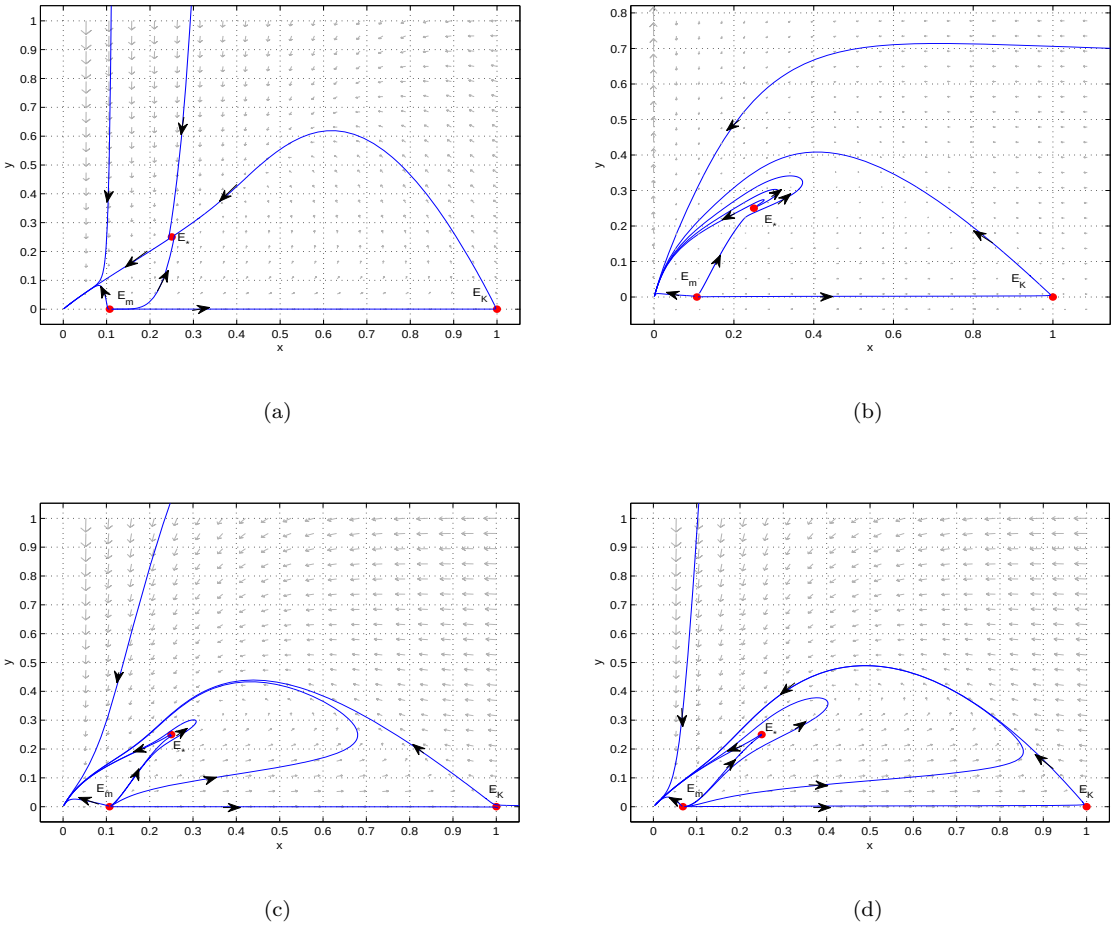

(a) (b)

(c) (d)

Figure 2. (a) E_* is an attracting saddle-node with $m = \frac{3}{28}$, $q = \frac{1}{4}$, $s = \frac{1}{2}$, $a = \frac{20}{7}$, (b) E_* is a repelling saddle-node with $m = \frac{3}{28}$, $q = \frac{1}{4}$, $s = \frac{1}{30}$, $a = \frac{20}{7}$, (c) E_* is a cusp of codimension 2 with $m = \frac{3}{28}$, $q = \frac{1}{4}$, $s = \frac{1}{16}$, $a = \frac{20}{7}$, (d) E_* is a cusp of codimension 3 with $m = \frac{3}{44}$, $q = \frac{23}{44}$, $s = \frac{23}{176}$, $a = \frac{4}{23}$.

and

$$\begin{aligned} G_1 &= G_{11}T + G_{12} \\ &= (-32q^5 - 128q^4 + 3392q^3 - 13184q^2 + 18688q - 8960)T - 32q^6 \\ &\quad + 4032q^4 - 25728q^3 + 62144q^2 - 65536q + 25344. \end{aligned}$$

Clearly, the sign of G is determined by that of G_1 for $\frac{1}{3} < q < 4 - 2\sqrt{3}$.

Define

$$\bar{G}_1 = (G_{11}\sqrt{q^2 - 8q + 8})^2 - (G_{12})^2 = 4096\left(q^4 + 16q^3 + 24q^2 - 64q + 16\right)(q-1)^4.$$

Using Sturm Theorem and Maple command "sturm", we obtain $q^4 + 16q^3 + 24q^2 - 64q + 16$ has no root for $\frac{1}{3} < q < 4 - 2\sqrt{3}$, which implies that $\bar{G}_1 \neq 0$. From the above analysis, we obtain that $G \neq 0$ for $\frac{1}{3} < q < 4 - 2\sqrt{3}$. Thus, E_* is a cusp of codimension three (see Figure 2(d)). The proof is completed. □

2.3. Bifurcation

In this section, we will analyse various possible bifurcations of system (2.1) and derive the conditions for saddle-node bifurcation, Bogdanov-Takens bifurcation and Hopf bifurcation.

2.3.1. Saddle-node bifurcation

From Lemma 2.2, as the parameter a changes, the number of equilibrium of system (2.1) will be changed. That is, when a crosses the threshold value $a_{SN} = a^*$, we can see that E_1 and E_2 are coincided by the occurrence of saddle-node bifurcation. We present the following theorem to illustrate the saddle-node bifurcation.

Theorem 2.4. *Choosing a as the bifurcation parameter, when a crosses the threshold value a_{SN}, system (2.1) undergoes a saddle-node bifurcation around E_*.*

Proof. Now we check the transversality condition for the occurrence of saddle-node bifurcation at $a = a_{SN}$ according to the Sotomayor's theorem [33].

Since

$$J_{E_*} = \begin{pmatrix} \dfrac{2mq}{m-q+1} & -\dfrac{2mq}{m-q+1} \\ s & -s \end{pmatrix},$$

we know J_{E_*} has a zero eigenvalue.

Assuming V and W represent eigenvectors corresponding to the zero eigenvalue of the matrices J_{E_*} and $J_{E_*}^T$, respectively, after straightforward computation, we have

$$V = \begin{pmatrix} V_1 \\ V_2 \end{pmatrix} = \begin{pmatrix} 1 \\ 1 \end{pmatrix},$$

$$W = \begin{pmatrix} W_1 \\ W_2 \end{pmatrix} = \begin{pmatrix} 1 \\ \dfrac{-2m}{s(m-q+1)} \end{pmatrix},$$

and

$$F_a(E_*, a_{SN}) = \begin{pmatrix} -\dfrac{4m^2}{(m-q+1)^2} \\ 0 \end{pmatrix},$$

$$D^2F(E_*; a_{SN})(V,V) = \begin{pmatrix} \dfrac{\partial^2 F_1}{\partial x^2}V_1^2 + 2\dfrac{\partial^2 F_1}{\partial x \partial y}V_1V_2 + \dfrac{\partial^2 F_1}{\partial y^2}V_2^2 \\ \dfrac{\partial^2 F_2}{\partial x^2}V_1^2 + 2\dfrac{\partial^2 F_2}{\partial x \partial y}V_1V_2 + \dfrac{\partial^2 F_2}{\partial y^2}V_2^2 \end{pmatrix}_{(E_*; a_{SN})}$$

$$= \begin{pmatrix} -\dfrac{2q\,(m-q+1)^2}{(m-1+q)\,(m-1-q)} \\ 0 \end{pmatrix}.$$

It is not difficult to see that V and W satisfy the transversality conditions

$$W^T F_a(E_*, a_{SN}) = -\frac{4m^2}{(m-q+1)^2} \neq 0,$$
$$W^T[D^2F(E_*; a_{SN})(V,V)] = -\frac{2q\,(m-q+1)^2}{(m-1+q)\,(m-1-q)} \neq 0.$$

Therefore, we conclude that when the parameter a cross critical value $a = a_{SN}$, system (2.1) undergoes a saddle-node bifurcation. The proof is completed. □

2.3.2. Degenerate Bogdanov-Takens bifurcation of codimension 3

When $s = s_1$, $a = a_*$, $m = m_*$, and $\frac{1}{3} < q < 4 - 2\sqrt{3}$, it follows from Theorem 2.3 (2.2) that the unique interior equilibrium E_* of system (2.1) is a cusp of codimension three. In the following, we will choose some proper bifurcation parameters to demonstrate the occurrence of Bogdognov-Taken bifurcation of codimension three around E_* under a small parameters perturbation. Then, we have the following theorem.

Theorem 2.5. *Assume that the conditions of Theorem 2.3 (2.2) hold. Choosing m, a and s as bifurcation parameters, system* (2.1) *undergoes a cusp type degenerate Bogdanov-Takens bifurcation of codimension three around E_*.*

Proof. Considering a, m, s as bifurcation parameters and substituting $s = s_1$, $a = a_*$ and $m = m_*$ into system (2.1), we have the following system

$$\begin{cases} \dot{x} = \dfrac{x(1-x)}{1+(a_*+\lambda_2)x}(x - m_* - \lambda_1) - qxy, \\ \dot{y} = (s_1+\lambda_3)y\Big(1 - \dfrac{y}{x}\Big), \end{cases} \tag{2.13}$$

where $\lambda = (\lambda_1, \lambda_2, \lambda_3)$ is in a small neighborhood of $(0,0,0)$.

Firstly, we make the following transformation to move the positive E_* to the origin,

$$x_1 = x - x_*,\ y_1 = y - y_*,$$

then system (2.13) becomes

$$\begin{cases} \dot{x}_1 = \bar{c}_{00} + \bar{c}_{10}x_1 + \bar{c}_{01}y_1 + \bar{c}_{20}x_1^2 + \bar{c}_{11}x_1y_1 + \bar{c}_{30}x_1^3 + \bar{c}_{40}x_1^4 + o(|x_1, y_1|^4), \\ \dot{y}_1 = \bar{d}_{10}x_1 + \bar{d}_{01}y_1 + \bar{d}_{20}x_1^2 + \bar{d}_{11}x_1y_1 + \bar{d}_{02}y_1^2 + \bar{d}_{30}x_1^3 + \bar{d}_{21}x_1^2y_1 \\ \qquad +\bar{d}_{12}x_1y_1^2 + \bar{d}_{40}x_1^4 + \bar{d}_{31}x_1^3y_1 + \bar{d}_{22}x_1^2y_1^2 + o(|x_1, y_1|^4), \end{cases} \tag{2.14}$$

where the coefficients are omitted for brevity.

Next, similarly to the transformations in [38, 39], we want to transform the system (2.13) to the universal unfolding of a cusp type degenerate Bogdanov-Takens of codimension 3. We make the following transformation

$$x_2 = x_1,\ \ y_2 = \bar{c}_{00} + \bar{c}_{10}x_1 + \bar{c}_{01}y_1 + \bar{c}_{20}x_1^2 + \bar{c}_{11}x_1y_1 + \bar{c}_{30}x_1^3 + \bar{c}_{40}x_1^4,$$

then system (2.14) becomes

$$\begin{cases} \dot{x}_2 = y_2, \\ \dot{y}_2 = \bar{e}_{00} + \bar{e}_{10}x_2 + \bar{e}_{01}y_2 + \bar{e}_{20}x_2^2 + \bar{e}_{11}x_2y_2 + \bar{e}_{02}y_2^2 + \bar{e}_{30}x_2^3 + \bar{e}_{21}x_2^2y_2 + \bar{e}_{12}x_2y_2^2 \\ \qquad +\bar{e}_{40}x_2^4 + \bar{e}_{31}x_2^3y_2 + \bar{e}_{22}x_2^2y_2^2 + o(|x_2, y_2|^4), \end{cases} \tag{2.15}$$

where $\bar{e}_{ij}$ can be represent by $\bar{c}_{ij}$ and $\bar{d}_{ij}$, and their detailed expressions are omitted for brevity. In the following proof of this theorem, all the coefficients of systems are also omitted.

(1) To eliminate y_2^2-term in system (2.15), making the following transformations successively,

$$x_2 = x_3 + \frac{\bar{e}_{02}}{2}x_3^2, \ y_2 = y_3 + \bar{e}_{02}x_3y_3,$$

system (2.15) becomes

$$\begin{cases} \dot{x}_3 = y_3, \\ \dot{y}_3 = \bar{f}_{00} + \bar{f}_{10}x_3 + \bar{f}_{01}y_3 + \bar{f}_{20}x_3^2 + \bar{f}_{11}x_3y_3 + \bar{f}_{30}x_3^3 + \bar{f}_{21}x_3^2y_3 \\ \qquad +\bar{f}_{12}x_3y_3^2 + \bar{f}_{40}x_3^4 + \bar{f}_{31}x_3^3y_3 + \bar{f}_{22}x_3^2y_3^2 + o(|x_3, y_3|^4). \end{cases} \tag{2.16}$$

(2) To eliminate $x_3y_3^2$-term and $x_3^2y_3^2$-term in system (2.16), making the transformations as follows

$$x_3 = X_4 + \frac{\bar{f}_{12}}{6}X_4^3, \quad y_3 = \left(1 + \frac{\bar{f}_{12}}{2}X_4^2\right)Y_4,$$
$$X_4 = x_4 + \frac{g_{22}}{12}x_4^4, \quad Y_4 = y_4 + \frac{g_{22}}{3}x_4^3y_4,$$

system (2.16) becomes

$$\begin{cases} \dot{x}_4 = y_4, \\ \dot{y}_4 = \bar{g}_{00} + \bar{g}_{10}x_4 + \bar{g}_{01}y_4 + \bar{g}_{20}x_4^2 + \bar{g}_{11}x_4y_4 + \bar{g}_{30}x_4^3 + \bar{g}_{21}x_4^2y_4 \\ \qquad +\bar{g}_{40}x_4^4 + \bar{g}_{31}x_4^3y_4 + o(|x_4, y_4|^4). \end{cases} \tag{2.17}$$

By calculation, we know

$$\bar{g}_{20} = -\frac{2q^2\,(q-2+T)\,(2q-3+T)}{(T+3q-4)\,(T+q-4)} + O(\lambda) < 0,$$

when $\frac{1}{3} < q < 4 - 2\sqrt{3}$, and $\lambda_1, \lambda_2, \lambda_3$ are sufficiently small.

(3) To eliminate x_4^3-term and x_4^4-term in system (2.17), making the transformations as follows

$$x_4 = x_5 - \frac{\bar{g}_{30}}{4\bar{g}_{20}}x_5^2 + \frac{15\bar{g}_{30} - 16\bar{g}_{20}\bar{g}_{40}}{80\bar{g}_{20}^2}x_5^3, \ y_4 = y_5,$$
$$d\tau = (1 + \frac{\bar{g}_{30}}{2\bar{g}_{20}}x_5 + \frac{48\bar{g}_{20}\bar{g}_{40} - 25\bar{g}_{30}^2}{80\bar{g}_{20}^2}x_5^2 + \frac{48\bar{g}_{20}\bar{g}_{30}\bar{g}_{40} - 35\bar{g}_{30}^3}{80\bar{g}_{20}^3}x_5^3)dt,$$

system (2.17) becomes (still denote τ by t):

$$\begin{cases} \dot{x}_5 = y_5, \\ \dot{y}_5 = \bar{h}_{00} + \bar{h}_{10}x_5 + \bar{h}_{01}y_5 + \bar{h}_{20}x_5^2 + \bar{h}_{11}x_5y_5 + \bar{h}_{21}x_5^2y_5 \\ \qquad +\bar{h}_{31}x_5^3y_5 + R(x_5, y_5, \lambda), \end{cases} \tag{2.18}$$

where

$$\begin{aligned} R(x_5, y_5, \lambda) = {} & y_5^2 O(|x_5, y_5|^2) + O(|x_5, y_5|^5) + O(\lambda)O(|y_5|^2) \\ & + O(|x_5, y_5|^3) + O(\lambda^2)O(|x_5, y_5|). \end{aligned} \tag{2.19}$$

(4) Removing the $x_5^2y_5$-term in system (2.18). Notice that

$$\bar{h}_{20} = -\frac{2q^2\,(q-2+T)\,(2q-3+T)}{(T+3q-4)\,(T+q-4)} + O(\lambda) < 0,$$

when $\frac{1}{3} < q < 4 - 2\sqrt{3}$, and $\lambda_1, \lambda_2, \lambda_3$ are sufficiently small. Let

$$x_5 = x_6,\ y_5 = y_6 + \frac{\bar{h}_{21}}{3\bar{h}_{20}}y_6^2 + \frac{\bar{h}_{21}^2}{36\bar{h}_{20}^2}y_6^3,\ d\tau = (1 + \frac{\bar{h}_{21}}{3\bar{h}_{20}}y_6 + \frac{\bar{h}_{21}^2}{36\bar{h}_{20}^2}y_6^2)dt,$$

then system (2.18) becomes

$$\begin{cases} \dot{x}_6 = y_6, \\ \dot{y}_6 = \bar{i}_{00} + \bar{i}_{10}x_6 + \bar{i}_{01}y_6 + \bar{i}_{20}x_6^2 + \bar{i}_{11}x_6y_6 + \bar{i}_{31}x_6^3y_6 + R_1(x_6, y_6, \lambda), \end{cases} \tag{2.20}$$

where $R(x_6, y_6, \lambda)$ has the same properties as (2.19).

(5) Convert the coefficients of x_6^2-term and $x_6^3y_6$-term in system (2.20) to 1 and -1, respectively. Notice that

$$\begin{aligned} \bar{i}_{20} &= -\frac{2q^2\,(q-2+T)\,(2q-3+T)}{(T+3q-4)\,(T+q-4)} + O(\lambda) < 0, \\ \bar{i}_{31} &= -\frac{q\,(q-2+T)^2\,Q}{40\,(2q-3+T)^2\,(T+q-4)^3\,(T+3q-4)^3} + O(\lambda), \end{aligned}$$

where

$$\begin{aligned} Q &= Q_1T + Q_2 \\ &= 320\left(q^5 + 4q^4 - 106q^3 + 412q^2 - 584q + 280\right)T \\ &\quad - 253440 + 320q^6 - 40320q^4 + 257280q^3 - 621440q^2 + 655360q. \end{aligned}$$

Define

$$\begin{aligned} \bar{Q} &= Q_1^2T^2 - Q_2^2 \\ &= -409600\left(q^4 + 16q^3 + 24q^2 - 64q + 16\right)(q-1)^4. \end{aligned}$$

Using Sturm's Thoerem and Maple command "sturm", we can obtain $\bar{Q}$ has no real root when $\frac{1}{3} < q < 4 - 2\sqrt{3}$, which implies that $Q \neq 0$. Then we have $\bar{i}_{31} \neq 0$ for $\frac{1}{3} < q < 4 - 2\sqrt{3}$.

Letting

$$x_6 = \bar{i}_{20}^{\frac{1}{5}}\bar{i}_{31}^{-\frac{2}{5}}x_7,\ y_6 = -\bar{i}_{20}^{\frac{4}{5}}\bar{i}_{31}^{-\frac{3}{5}}y_7,\ d\tau = -\bar{i}_{20}^{-\frac{3}{5}}\bar{i}_{31}^{\frac{1}{5}}dt,$$

and still denoting τ as t, system (2.20) becomes

$$\begin{cases} \dot{x}_7 = y_7, \\ \dot{y}_7 = \bar{j}_{00} + \bar{j}_{10}x_7 + \bar{j}_{01}y_7 + \bar{j}_{11}x_7y_7 - x_7^2 + x_7^3y_7 + R_2(x_7, y_7, \lambda), \end{cases} \tag{2.21}$$

where $R_2(x_7, y_7, \lambda)$ has the same properties as (2.19).

(6) Removing the x_7-term in system (2.21). Let $x_7 = X - \frac{\bar{j}_{20}}{2}$ and $y_7 = Y$. Thus, system (2.21) is equivalent to the following system

$$\begin{cases} \dot{X} = Y, \\ \dot{Y} = \mu_1 + \mu_2Y_1 + \mu_3XY + X^2 - X^3Y + R_3(X, Y, \lambda), \end{cases} \tag{2.22}$$

where $R_3(X, Y, \lambda)$ has the same properties as (2.19).

After calculation, we get

$$B_2 = \left|\frac{\partial(\mu_1, \mu_2, \mu_3)}{\partial(\lambda_1, \lambda_2, \lambda_3)}\right|_{\lambda=0} = \frac{B_{21}}{\eta q^5(2q-3+T)^2(q-2+T)^{\frac{24}{5}}(T+q-4)^3(T+3q-4)Q^{\frac{1}{5}}},$$

where η is a nonzero constant, and

$$\begin{aligned} B_{21} =& B_{210}T + B_{211} \\ =& (-460800q^{10} + 5222400q^9 + 39321600q^8 - 1002086400q^7 \\ &+ 7443763200q^6 - 29473382400q^5 + 70187212800q^4 \\ &- 103687526400q^3 + 93120000000q^2 - 46606540800q + 9976627200)T \\ &- (460800q^9 - 3379200q^8 - 50995200q^7 + 791961600q^6 - 4500787200q^5 \\ &+ 13741056000q^4 - 24575385600q^3 + 25786214400q^2 - 14714265600q \\ &+ 3527270400)(q^2 - 8q + 8). \end{aligned}$$

By simple calculation, we get that $(2q-3+T)(q-2+T)(T+q-4)(T+3q-4) \neq 0$ when $\frac{1}{3} < q < 4 - 2\sqrt{3}$. Obviously, $Q \neq 0$ for $\frac{1}{3} < q < 4 - 2\sqrt{3}$. For B_{21} we have

$$\begin{aligned} \bar{B}_{21} =& B_{210}^2T^2 - B_{211}^2 \\ =& 94371840000\left(q^2 - 8q + 8\right)(3q-1)\left(q^4 + 16q^3 + 24q^2 - 64q + 16\right)(q-1)^8. \end{aligned}$$

Using Sturm's Theorem and Maple command "sturm" again, we obtain $\bar{B}_{21} \neq 0$ for $\frac{1}{3} < q < 4 - 2\sqrt{3}$, that is $B_2 \neq 0$ for $\frac{1}{3} < q < 4 - 2\sqrt{3}$.

By the results of [9], system (2.22) is the versal unfolding of Bogdanov-Takens singularity (cusp case) of codimension three. Hence, system (2.1) undergoes a Bogdanov-Takens bifurcation of codimension three when the parameters λ_1, λ_2 and λ_3 vary in a small neighborhood of $(0, 0, 0)$. The proof is completed. □

Now, we give several sets of numerical simulations to verity the occurrence of Bogdanov-Takens bifurcation of codimension three. Fixing $(a, s) = (\frac{4}{23}, \frac{553}{4400})$, and using Matcont, we obtain

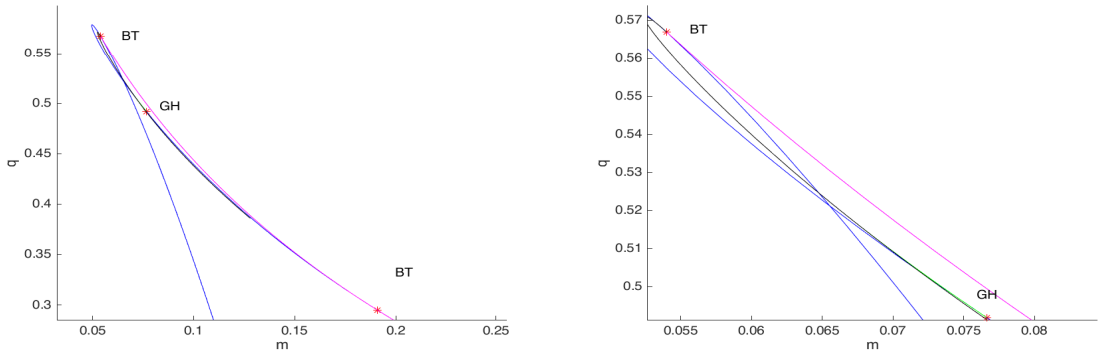

(a) $(a, s) = (\frac{4}{23}, \frac{553}{4400})$ (b) Local amplified phase portrait of (a)

Figure 3. Bifurcation diagram of cusp type degenerate Bogdanov-Takens bifurcation of codimension 3 for system (2.1) in the (m, q) plane. The blue, green, black and magenta solid lines represent Hopf bifurcation, degenerate Hopf bifurcation, homoclinic bifurcation and saddle-node bifurcation, respectively.

Table 1. Dynamic behaviors in Figure 3 with $(a, s) = \left(\frac{4}{23}, \frac{553}{4400}\right)$, where "SF", "S" and "UF" denote "stable focus", "saddle" and "unstable focus", respectively.

q	m	E_1	E_2	Limit cycle and homoclinic loop
0.45	0.094	S	SF	No (Figure 4(a))
	0.09424	S	SF	A homoclinic loop (Figure 4(b))
	0.0946	S	SF	An unstable limit cycle (Figure 4(c))
	0.096	S	UF	No (Figure 4(d))
0.5045	0.0716	S	SF	No (Figure 5(a))
	0.0717	S	UF	A stable limit cycle (Figure 5(b))
	0.071735045	S	UF	A stable limit cycle and a homoclinic loop (Figure 5(c))
	0.071737	S	UF	A stable limit cycle and an unstable limit cycle (Figure 5(d))
	0.07175	S	UF	No (Figure 5(e))

the bifurcation diagram of system (2.1) as shown in Figure 3. Further, we list the detail dynamics of system (2.1) with different parameters q and m in Table 1 and Figures 4-5.

(1) From Table 1 and Figure 4, when $q = 0.45$, system (2.1) successively undergoes a subcritical Hopf bifurcation and a homoclinic bifurcation.

During this transition, system (2.1) exhibits both a homoclinic loop and an unstable limit cycle Figure 4(c).

(2) From Table 1 and Figure 5, for $q = 0.5045$, the system exhibits much richer dynamics. That is system (2.1) successively undergoes a supercritical Hopf bifurcation, a homoclinic bifurcation and a saddle-node bifurcation of limit cycle. Especially, when $m = 0.071735045$, a homoclinic loop connected to the saddle E_1 coexists with a stable limit cycle Figure 5(c). Further as m increases, the system advents both a stable inner limit cycle and an unstable outer limit cycle Figure 5(d), forming a bistable regime. Eventually, both limit cycles vanish Figure 5(e).

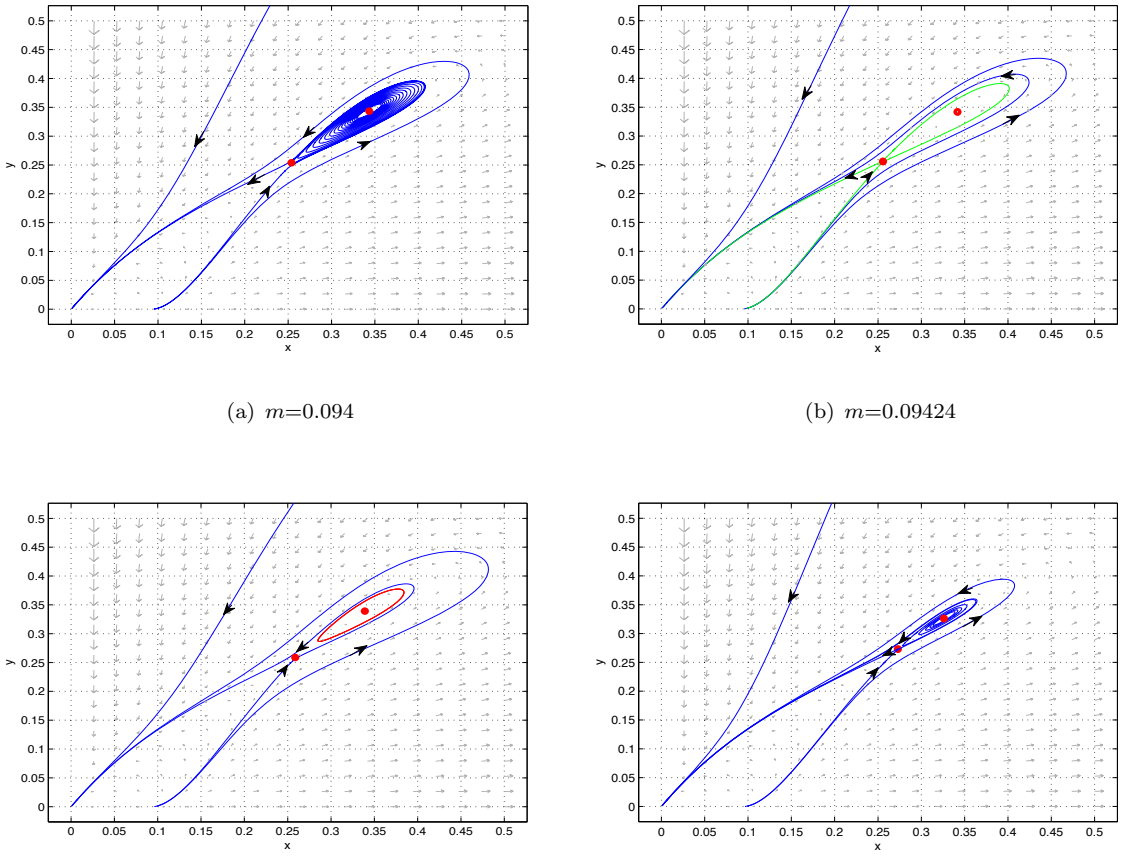

(a) m=0.094 (b) m=0.09424

(c) m=0.0946 (d) m=0.096

Figure 4. Phase portraits of system (2.1) with $(a, s, q) = \left(\frac{4}{23}, \frac{553}{4400}, 0.45\right)$.

2.3.3. Degenerate Hopf bifurcation of codimension 4

From Theorem 2.2, the stability of positive equilibrium E_2 of system (2.1) can be changed, which means that Hopf bifurcation may occur around E_2. For simplicity, we denote x_2 by z. From $F(z) = 0$ and $Tr(J_{E_2}) = 0$, we have

$$a = \bar{a} = \frac{((1-z)(z-m) - qz)}{qz^2}, \ s = \bar{s} = \frac{qz(qz - z^2 + m)}{(1-z)(z-m)},$$

and

$$Det(J_{E_2}) = z^2(qz - z^2 + m)((m+1)z - 2m - qz).$$

By $\bar{a} > 0$, $\bar{s} > 0$ and $Det(J_{E_2}) > 0$, we obtain $(m, z, q) \in \Omega = \Omega_1 \cup \Omega_2$,

$$\Omega_1 := \left\{(m, z, q) | \, 0 < m < 1, \frac{2m}{m+1} < z \leq \sqrt{m}, 0 < q < \frac{(m+1)z - 2m}{z}\right\},$$

$$\Omega_2 := \left\{(m, z, q) | \, 0 < m < 1, \sqrt{m} < z < \frac{m+1}{2}, \frac{z^2 - m}{z} < q < \frac{(1-z)(z-m)}{z}\right\}.$$

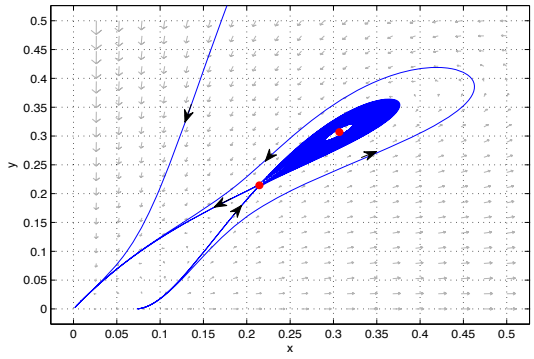

(a) m=0.0716

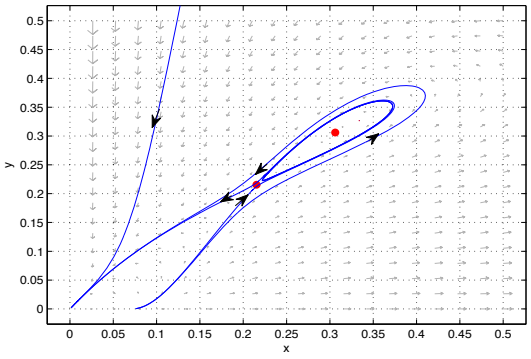

(b) m=0.0717

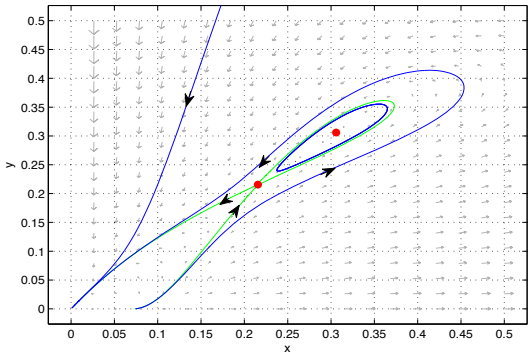

(c) m=0.071735045

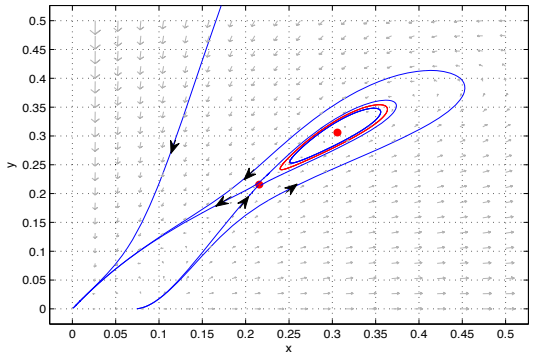

(d) m=0.071737

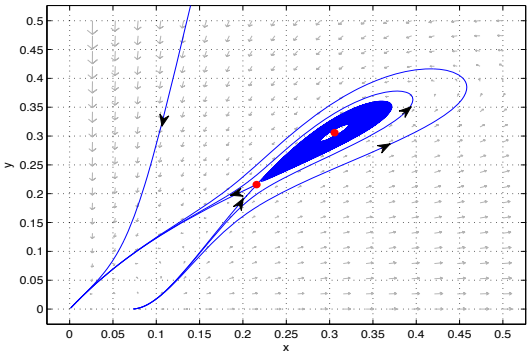

(e) m=0.07175

Figure 5. Phase portraits of system (2.1) with $(a, s, q) = \left(\frac{4}{23}, \frac{553}{4400}, 0.5045\right)$.

In order to obtain the focal values of $E_2(z, z)$, we make the following transformations successively

$$x = x_1 + z,\ y = y_1 + z,\ \tau_1 = x(1 + ax)t,$$

$$x_1 = -x_2\frac{a_{10}a_{01}}{a_{10}^2+D_0} - y_2\frac{a_{01}\sqrt{D_0}}{a_{10}^2+D_0},\ y_1 = x_2,\ \tau_2 = \sqrt{D_0}\tau_1,$$

where

$$a_{10} = z(qz-z^2+m),\ a_{01} = (1-z)(m-z)z,\ b_{10} = z(qz-z^2+m),\ b_{01} = -z(qz-z^2+m),$$
$$D_0 = a_{10}b_{01} - a_{01}b_{10} = Det(J_{E_2}),$$

then system (2.1) becomes (still rewriting τ_2 by t)

$$\begin{cases} \dot{x}_2 = y_2 + c_{11}x_2y_2 + c_{02}y_2^2 + c_{21}x_2^2y_2 + c_{12}x_2y_2^2, \\ \dot{y}_2 = -x_2 + d_{20}x_2^2 + d_{11}x_2y_2 + d_{02}y_2^2 + d_{30}x_2^3 + d_{21}x_2^2y_2 + d_{12}x_2y_2^2 \\ \qquad +d_{03}y_2^3 + d_{40}x_2^4 + d_{31}x_2^3y_2 + d_{22}x_2^2y_2^2 + d_{13}x_2y_2^3 + d_{04}y_2^4, \end{cases}$$

for brevity, whose coefficients are omitted here. From [35,36,41], we get the first four Lyapunov numbers as follows

$$L_1 = \frac{zf_1}{8D_0^{\frac{3}{2}}(m-z)(z-1)},$$
$$L_2 = -\frac{z^3f_2}{288D_0^{\frac{7}{2}}(m-z)^2(z-1)^2},$$
$$L_3 = -\frac{z^5f_3}{663552D_0^{\frac{11}{2}}(m-z)^3(z-1)^3},$$
$$L_4 = -\frac{z^7f_4}{238878720D_0^{\frac{15}{2}}(m-z)^4(z-1)^4},$$

where

$$\begin{aligned} f_1 = &-m^3z^5 - m^2q^2z^4 + m^2q\,z^5 + 2m^2z^6 + 2m\,q^3z^4 - 2mq\,z^6 - m\,z^7 - q^4z^4 + q\,z^7 \\ &+ 3m^2q^2z^3 - m^2q\,z^4 - 11m^2z^5 - 4m\,q^3z^3 - m\,q^2z^4 + 3mq\,z^5 + 7m\,z^6 + 2q^3z^4 \\ &- 2q\,z^6 - z^7 + m^4z^2 - m^3q\,z^2 - 9m^3z^3 - 3m^2q^2z^2 + m^2q\,z^3 + 17m^2z^4 \\ &- mq\,z^4 - 11m\,z^5 - q^2z^4 + q\,z^5 + 2z^6 - 2m^4z + m^3qz + 7m^3z^2 - m^2q\,z^2 \\ &+ 5m\,z^4 - z^5 + m^4 - 2m^3z + m^2z^2 + 5m^3z^4 + 3m\,q^2z^3 - 9m^2z^3, \end{aligned}$$

the detailed expressions of f_2, f_3 and f_4 are omitted here for brevity.

The algebraic variety $V(f_1,f_2,f_3)$ denotes the common zero roots of f_i $(i=1,2,3)$. lcoeff(f,x) represents the leading coefficient of the polynomial f with respect to x. For the polynomial $f(x,y)$, let $f^+(x,y)$ and $f^-(x,y)$ be the summations of the positive and negative terms in $f(x,y)$ respectively [28].

It is obvious that the denominators of L_i are not zeros for $(m,z,q)\in\Omega$, thus $V(L_1,L_2,L_3)\cap\Omega = V(f_1,f_2,f_3)\cap\Omega$. The following resultants has been calculated by using Maple software

$$\text{res}(f_1,f_2,q) = 1296m^3z^{40}(z-1)^{18}(m-z)^{18}S_1S_2^2g_1,$$
$$\text{res}(f_1,f_3,q) = -5308416m^4z^{62}(z-1)^{26}(m-z)^{26}S_1S_2^2g_2,$$

$$\begin{aligned}
&\operatorname{res}(f_2, f_3, q) = -99179645184m^9z^{142}(z-1)^{54}(m-z)^{54}S_1S_2^2g_3,\\
&\operatorname{res}(g_1, g_2, z) = c_1m^{220}(8m-1)^3(m-8)^3(m+1)^{11}(m-1)^{32}R_1R_2h_1,\\
&\operatorname{res}(g_1, g_3, z) = c_2m^{554}(8m-1)^3(m-8)^3(m+1)^{11}(m-1)^{96}R_1R_2h_2,
\end{aligned}$$

where

$$\begin{aligned}
&S_1 = (4-z)m - z,\\
&S_2 = z(1-z) - (3-z)m,\\
&R_1 = m^4 + 52m^3 + 166m^2 + 52m + 1,
\end{aligned}$$

c_1, c_2 are nonzero constants, $g_i\,(i=1,2,3)$ are polynomials in m and z, h_1, h_2, R_2 are polynomials of m with degree 258, 806, 40, respectively. To save space, we omit the detailed expressions of them.

By computation, we have

$$\begin{aligned}
&l_1 = \operatorname{lcoeff}(f_1, q) = -z^4, \quad l_2 = \operatorname{lcoeff}(f_2, q) = 9z^9,\\
&l_3 = \operatorname{lcoeff}(g_1, z) = 2(8m-1)(m-8)(m+1).
\end{aligned}$$

Lemma 2.3. *Assume $(m, z, q) \in \Omega$ holds, then $V(f_1, f_2, f_3, l_i) \cap \Omega = \emptyset\,(i = 1, 2, 3)$.*

Proof. Obviously, $l_1 < 0$, $l_2 > 0$, that is $V(f_1, f_2, f_3, l_i) \cap \Omega = \emptyset\,(i = 1, 2)$.

Next, we have $V(f_1, f_2, f_3, l_3) \cap \Omega = V(f_1, f_2, f_3, 8m-1) \cap \Omega$. Note that $(m, z, q) \in \Omega$. When $m = \frac{1}{8}$, we have $\Omega = \bar{\Omega}_1 \cup \bar{\Omega}_2$,

$$\begin{aligned}
\bar{\Omega}_1 &:= \left\{(z,q) \middle| \frac{2}{9} < z \le \frac{\sqrt{2}}{4}, 0 < q < \frac{9z-2}{8z}\right\},\\
\bar{\Omega}_2 &:= \left\{(z,q) \middle| \frac{\sqrt{2}}{4} < z < \frac{9}{16}, \frac{8z^2-1}{8z} < q < \frac{(1-z)(8z-1)}{8z}\right\}.
\end{aligned}$$

Substituting $m = \frac{1}{8}$ into f_1, f_2, f_3, we get

$$f_1 = \frac{f_{11}}{4096}, \quad f_2 = -\frac{f_{12}}{134217728}, \quad f_3 = \frac{f_{13}}{4398046511104},$$

where

$$\begin{aligned}
f_{11} = {} & -4096q^4z^4 + 4096q\,z^7 + 9216q^3z^4 - 9216q\,z^6 - 4608z^7 - 2048q^3z^3 - 4672q^2z^4\\
& + 5696q\,z^5 + 11904z^6 + 1728q^2z^3 - 576q\,z^4 - 10440z^5 - 192q^2z^2 + 64q\,z^3\\
& + 3688z^4 - 72q\,z^2 - 648z^3 + 8qz + 121z^2 - 18z + 1,
\end{aligned}$$

and the expressions of f_{12}, f_{13} are omitted for brevity.

Obviously, $V(f_1, f_2, f_3, 8m-1) \cap \Omega = V(f_{11}, f_{12}, f_{13}) \cap \Omega$. By calculation, we have the following results

$$\begin{aligned}
&\operatorname{res}(f_{11}, f_{12}, q) = c_5z^{40}(9z-4)\left(8z^2-9z+3\right)^2(8z-1)^{18}(z-1)^{18}g_{11},\\
&\operatorname{res}(f_{11}, f_{13}, q) = c_6z^{62}(9z-4)\left(8z^2-9z+3\right)^2(8z-1)^{26}(z-1)^{26}g_{12},\\
&\operatorname{res}(g_{11}, g_{12}, z) \neq 0,
\end{aligned}$$

where c_5, c_6 are nonzero constants, and we omit the expressions of g_{11}, g_{12} there for brevity.

Note that $\frac{2}{9} < z < \frac{9}{16}$, then $(8z^2 - 9z + 3)(8z - 1)(z - 1) \neq 0$. Obviously, $\mathrm{lcoeff}(f_{11}, q) = -4096z^4 \neq 0$. According to Lemma 2 in [8], we get

$$V(f_{11}, f_{12}, f_{13}) \cap \Omega = \{V(f_{11}, f_{12}, f_{13}, 9z - 4) \cup V(f_{11}, f_{12}, f_{13}, g_{11}, g_{12})\} \cap \Omega.$$

Because $\mathrm{res}(g_{11}, g_{12}, z) \neq 0$, we have $V(f_{11}, f_{12}, f_{13}, g_{11}, g_{12}) \cap \Omega = \emptyset$. Substituting $z = \frac{4}{9}$ into f_{11}, f_{12} and Ω, we get

$$f_{11} = -\frac{(288q - 47)f_{111}}{4782969}, \quad f_{12} = \frac{2(288q - 47)f_{122}}{1853020188851841}, \quad \frac{47}{288} < q < \frac{115}{288},$$

where

$$\begin{aligned} f_{111} &= 2654208q^3 - 2552832q^2 + 721280q - 119025, \\ f_{122} &= 2629465015396073472q^8 - 9160520481877524480q^7 + 12227377243273297920q^6 \\ &\quad - 7118161454510899200q^5 + 967311804727296000q^4 + 799260921255002112q^3 \\ &\quad - 400451183005711360q^2 + 93247072677903600q - 14979637254839625. \end{aligned}$$

Since $\mathrm{res}(f_{111}, f_{122}, q) \neq 0$, we have $V(f_{11}, f_{12}, f_{13}, 9z - 4) \cap \Omega = \emptyset$. This indicates that $V(f_1, f_2, f_3, l_3) \cap \Omega = \emptyset$.

From the above analysis, we obtain that $V(f_1, f_2, f_3, l_i) \cap \Omega = \emptyset\, (i = 1, 2, 3)$. The proof is completed. □

Now, in the following, we show that $V(f_1, f_2, f_3) \cap \Omega \neq \emptyset$ and $V(f_1, f_2, f_3, f_4) \cap \Omega = \emptyset$.

Step I. Simplifying the semi-algeraic variety $V(f_1, f_2, f_3)$.

According to Lemma 2 in [8] and Lemma 2.3, we have the following decomposition

$$V(f_1, f_2, f_3) \cap \Omega = \{V_1 \cup V_2 \cup V_3 \cup V_4 \cup V_5\} \cap \Omega,$$

where

$$\begin{aligned} &V_1 = V(f_1, f_2, f_3, S_1), \quad V_2 = V(f_1, f_2, f_3, S_2), \\ &V_3 = V(f_1, f_2, f_3, g_1, g_2, g_3, 8m - 1), \quad V_4 = V(f_1, f_2, f_3, g_1, g_2, g_3, R_2), \\ &V_5 = V(f_1, f_2, f_3, g_1, g_2, g_3, h_1, h_2). \end{aligned}$$

Step II. Proving that $V_i \cap \Omega = \emptyset$ $(i = 1, 2)$.

Obviously, $S_1 = 0$ has a unique root $m = \frac{z}{4-z}$. Substituting $m = \frac{z}{4-z}$ into $f_i\, (i = 1, 2, 3)$ and Ω, we get

$$\begin{aligned} f_1 &= \frac{z^4((z-4)\,q - z^2 + 4z - 1)f_{21}}{(4-z)^4}, \quad f_2 = \frac{z^9((z-4)\,q - z^2 + 4z - 1)f_{22}}{(4-z)^9}, \\ f_3 &= \frac{z^{14}((z-4)\,q - z^2 + 4z - 1)f_{23}}{(4-z)^{14}}, \\ \underline{\Omega}_1 &= \left\{(z, q) |\, 0 < z \leq 2 - \sqrt{3},\, 0 < q < \frac{2}{4-z}\right\}, \\ \underline{\Omega}_2 &= \left\{(z, q) |\, 2 - \sqrt{3} < z < 2 - \sqrt{2},\, \frac{z^2 - 4z + 1}{z - 4} < q < \frac{(1-z)(3-z)}{z-4}\right\}, \end{aligned}$$

where $\Omega = \underline{\Omega}_1 \cup \underline{\Omega}_2$, and

$$f_{21} = (z-4)^3q^3 + (z^2-4z+5)(z-4)^2q^2 + (z-1)(z-3)(z-4)(z-2)^2q + (z-1)^2(z-3)^2,$$

the expressions of f_{22}, f_{23} are omitted for brevity. In addition, Note that $(z-4)\,q - z^2 + 4z - 1 \neq 0$ for $m = \frac{z}{4-z}$ and $(m, z, q) \in \Omega$. Thus, $V_1 \cap \Omega = V(f_{21}, f_{22}, f_{23}) \cap \Omega$. By calculation, we have

$$\begin{aligned}
&\operatorname{res}(f_{21}, f_{22}, q) = 216\left(z^2-4z+1\right)^2(z-1)^{12}(z-3)^{12}(z-4)^{24}g_{21},\\
&\operatorname{res}(f_{21}, f_{23}, q) = 110592\left(z^2-4z+1\right)^2(z-1)^{17}(z-3)^{17}(z-4)^{39}g_{22},\\
&\operatorname{res}(g_{21}, g_{22}, z) \neq 0,
\end{aligned}$$

and the expressions of g_{21}, g_{22} are omitted for brevity. Obviously, $(z-1)(z-3)(z-4) \neq 0$ and $\operatorname{lcoeff}(f_{21}, q) = (z-4)^3 \neq 0$ in Ω. Then, according to Lemma 2 of [8], we get

$$V(f_{21}, f_{22}, f_{23}) \cap \Omega = \left\{V(f_{21}, f_{22}, f_{23}, z^2-4z+1) \cup V(f_{21}, f_{22}, f_{23}, g_{21}, g_{22})\right\} \cap \Omega.$$

From $\operatorname{res}(g_{21}, g_{22}, z) \neq 0$, we have $V(f_{21}, f_{22}, f_{23}, g_{21}, g_{22}) \cap \Omega = \emptyset$. For $z^2 - 4z + 1 = 0$, we get $z = 2 - \sqrt{3}$. Substituting this into Ω, we obtain $m = 7 - 4\sqrt{3}$, $0 < q < 4 - 2\sqrt{3}$ and

$$f_{21} = (15\sqrt{3}+26)(q^2 - (4-2\sqrt{3})q + 14 - 8\sqrt{3})(4 - 2\sqrt{3} - q) > 0,$$

which implies that E_2 is a weak focus of order one. Therefore, the above discussion demonstrates that $V(f_{21}, f_{22}, f_{23}) \cap \Omega = \emptyset$, that is $V_1 \cap \Omega = \emptyset$.

Using the method similar to the above, we can prove that $V_2 \cap \Omega = \emptyset$.

Step III. Proving that $V_3 \cap \Omega = \emptyset$.

Note that $V_3 \subseteq V(f_1, f_2, f_3, 8m-1)$. Similar to the proof of Lemma 2.3, we can obtain $V(f_1, f_2, f_3, 8m-1) \cap \Omega = \emptyset$. Hence, $V_3 \cap \Omega = \emptyset$.

Step IV. Proving that $V_5 \cap \Omega = \emptyset$.

We have $\operatorname{res}(h_1, h_2, m) \neq 0$, and $V_5 \subseteq V(h_1, h_2)$, thus, $V_5 \cap \Omega = \emptyset$.

Step V. Proving that $V_4 \cap \Omega \neq \emptyset$ and $V(f_1, f_2, f_3, f_4) \cap \Omega = \emptyset$.

Lemma 2.4. *Assume that $(m, z, q) \in \Omega$ holds, we obtain $V_4 \cap \Omega \neq \emptyset$ and $V(f_1, f_2, f_3, f_4) \cap \Omega = \emptyset$.*

Proof. Note that

$$V_4 = V(f_1, g_1, R_2) \cap V(f_2, f_3, g_2, g_3).$$

We get the common real roots of $\{f_1, g_1, R_2\}$ in Ω, and verify whether these roots are also the common real roots of $\{f_1, f_2, f_3\}$ or $\{f_1, f_2, f_3, f_4\}$ in Ω. In the following discussion, we mainly use the real root isolation algorithm of multivariate polynomial systems [28].

According to isolating the real roots of $R_2(z)$, using the command "realroot", we get the following two real roots $M_i \in [\underline{M}_i, \overline{M}_i]\,(i = 1, 2)$ in Ω, where

$$\begin{aligned}
\underline{M}_1 &= \frac{1610105768535767049126415679163681426400158660535353066973725686563816043148388654238 7}{7957171782556586274486115970349133441607298412757563479047423630290551952200534008528896},\\
\overline{M}_1 &= \frac{8050528842678835245632078395818407132000793302676765334868628432819080215741943271315}{3978585891278293137243057985174566720803649206378781739523711815145275976100267004264448},\\
\underline{M}_2 &= \frac{4971553352347499678031575273235355005704297382106327378514523166574888772793732695010769 55}{4074071952668972172536891376818756322102936787331872501272280898708762599526673412366794752},
\end{aligned}$$

$$\overline{M}_2 = \frac{39772426818779997424252602185882840045634379056850619028116185332599110182349861560086163693259257562135177738029513101455005057682349429865498001017824718967010079621338729893435801 6}.$$

For the real root interval $[\underline{M}_1, \overline{M}_1]$ of R_2, using the "realroot" again, we get three positive real roots isolation intervals of $\{R_2(m), g_1(m,z)\}$ as follows

$$\underline{Z}_1 = \frac{17001700610065517794908124122722505501517969179950071272020081164950338598539936962066715914343565113172548972231940698266883214596825515126958094847260581103904401068017057792},$$
$$\overline{Z}_1 = \frac{17001700610065517794908124122722505501517969179950071272020081164950338598539936972904515914343565113172548972231940698266883214596825515126958094847260581103904401068017057792},$$
$$\underline{Z}_2 = \frac{65525068732295161299810171071738800471008859211932720167355187899320634040837163792774389}{40740719526689721725368913768187563221029367873318725012722808987087625995266734123667947 52},$$
$$\overline{Z}_2 = \frac{65525068732295161299810171071738800471008859211932720167355187899320634040837163804476297}{40740719526689721725368913768187563221029367873318725012722808987087625995266734123667947 52},$$

where we omit the expression of Z_3.

For the real root isolation interval $[\underline{M}_1, \overline{M}_1] \times [\underline{Z}_1, \overline{Z}_1]$ of $\{R_2(m), g_1(m,z)\}$, f_1 has a unique positive real root isolation interval as follows

$$\underline{Q}_1 = \frac{135635251979561620214383085600552535482679819775578833921141504568183984734836715276070840288205403346623318458823496583257521372037936003911913780434075891266276556 8},$$
$$\overline{Q}_1 = \frac{542541007918246480857532342402210141930719279102315335684566018272735938939346863512428336115282161338649327383529398633303008548815174401564765512173630356506510622 72}.$$

By Theorem 2.2 of [28], we have $f_2(M_1, Z_1, Q_1) < f_2^+(\overline{M}_1, \overline{Z}_1, \overline{Q}_1) + f_2^-(\underline{M}_1, \underline{Z}_1, \underline{Q}_1) \approx -9.471463745 \times 10^{-21}$, which implies that (M_1, Z_1, Q_1) is not the common positive real root of $\{f_1, f_2\}$. Then E_2 is a weak focus of order 2 when $(m,z,q) = (M_1, Z_1, Q_1)$.

For the real root isolation interval $[\underline{M}_1, \overline{M}_1] \times [\underline{Z}_2, \overline{Z}_2]$ of $\{R_2(m), g_1(m,z)\}$, f_1 has a unique positive real root isolation interval as follows

$$\underline{Q}_2 = \frac{14086778198230952628145592433565125568692031350946662392999487103998306244446934675245891591434356511317254897223194069826688321459682551512695809484726058110390440106801705779 2},$$
$$\overline{Q}_2 = \frac{70433890991154763140727962167825627843460156754733311964997435519991531222234673376265979571717825565862744861159703491334416072984127575634790474236302905519522005340085289 96}.$$

Similar to the above calculation, we obtain that (M_1, Z_2, Q_2) is a common positive real root of $\{f_1, f_2, f_3\}$.

That is $V_4 \cap \Omega \neq \emptyset$. In the other hand, we get $f_4(M_1, Z_2, Q_2) < f_4^+(\overline{M}_1, \overline{Z}_2, \overline{Q}_2) + f_4^-(\underline{M}_1, \underline{Z}_2, \underline{Q}_2) \approx -5.108043632 \times 10^{-36}$, which implies that (M_1, Z_2, Q_2) is not the real root of f_4. Thus, $V(f_1, f_2, f_3, f_4) \cap \Omega = \emptyset$ and E_2 is a weak focus of order 4 when $(m,z,q) = (M_1, Z_2, Q_2)$, where $M_1 \approx 0.002023465$, $Z_2 \approx 0.016083434$, $Q_2 \approx 0.088516238$.

For the real root isolation interval $[\underline{M}_1, \overline{M}_1] \times [\underline{Z}_3, \overline{Z}_3]$. By Theorem 2.2 of [28], we can show that (M_1, Z_3) is not a common zero of $\{R_2(m), g_1(m,z)\}$ in Ω, since $g_1(M_1, Z_3) > g_1^-(\overline{M}_1, \overline{Z}_3) + g_1^+(\underline{M}_1, \underline{Z}_3) \approx 1.749042283 \times 10^{-25}$.

Similar to the above analysis, $\{f_1, f_2, f_3\}$ has no common real root in $[\underline{M}_2, \overline{M}_2]$. Then $V(f_1, f_2, f_3) \cap \Omega \neq \emptyset$ and $V(f_1, f_2, f_3, f_4) \cap \Omega = \emptyset$. The proof is completed. □

Define

$$\begin{aligned}
W_1 &:= \{(m,z,q) \in \Omega : f_1(m,z,q) \neq 0\}, \\
W_2 &:= \{(m,z,q) \in \Omega : f_1(m,z,q) = 0, f_2(m,z,q) \neq 0\}, \\
W_3 &:= \{(m,z,q) \in \Omega : f_1(m,z,q) = 0, f_2(m,z,q) = 0, f_3(m,z,q) \neq 0\}, \\
W_4 &:= \{(m,z,q) \in \Omega : f_1(m,z,q) = 0, f_2(m,z,q) = 0, f_3(m,z,q) = 0\}.
\end{aligned}$$

From Lemma 2.4, E_2 is a weak focus of order 2 (or 4) for $(m,z,q) = (M_1, Z_1, Q_1)$ (or (M_1, Z_2, Q_2)), that is $W_2 \neq \emptyset$ and $W_4 \neq \emptyset$. When $m = \frac{3}{1000}$, we give the following Lemma to show that $W_3 \neq \emptyset$.

Define

$$\Omega_{1*} := \left\{ (z,q) \,\middle|\, \frac{6}{1003} < z \le \frac{\sqrt{30}}{100},\ 0 < q < \frac{1003z-6}{1000z} \right\},$$
$$\Omega_{2*} := \left\{ (z,q) \,\middle|\, \frac{\sqrt{30}}{100} < z < \frac{1003}{2000},\ \frac{1000z^2-3}{1000z} < q < \frac{(1-z)(1000z-3)}{1000z} \right\},$$
$$\Omega_* = \Omega_{1*} \cup \Omega_{2*}.$$

Lemma 2.5. *Assume that* $(a,s) = (\bar{a},\bar{s})$. *If* $(m,z,q) = (\frac{3}{1000}, P_2, K_2)$, *then* E_2 *is a weak focus of order* 3, *where* $P_2 \approx 0.022193491$, $K_2 \approx 0.084731655$.

Proof. Note that $(m,z,q) \in \Omega$. Substituting $m = \frac{3}{1000}$ into Ω, we get $(z,q) \in \Omega_*$. Using the command "realroot", we get that $g_1(\frac{3}{1000}, z)$ exists three positive real roots isolation intervals $P_i \in [\underline{P}_i, \overline{P}_i]$ $(i = 1,2,3)$ in Ω_*. Here, we only consider $P = P_2$ where

$$\underline{P}_2 = \frac{39766204281731781859283414758351146751240442274671901122481670439227104644853921180093299525532759871 3}{17917957937422433684459538244547554224973163977877196279199912807710334969441287563047019946172856926208},$$
$$\overline{P}_2 = \frac{79532408563463563718566829516702293502480884549343802244963340878454209289707842360186599051065519961 3}{35835915874844867368919076489095108449946327955754392558399825615420669938882575126094039892345713852416}.$$

For the real root interval $[\underline{P}_2, \overline{P}_2]$, using the real root isolation algorithm of multivariate polynomial systems [28], we obtain a unique positive real root isolation interval $K_2 \in [\underline{K}_2, \overline{K}_2]$ of f_1 in Ω_*, where

$$\underline{K}_2 = \frac{32921109955181755092053255118136827509672646156585977279363913321319895196334377 4871}{38853377844514581418389238136470378132848136781042790425036248194778085704104169963 52},$$
$$\overline{K}_2 = \frac{16460554977590877546026627559068413754836323078292988639681956660659947598167188755 7}{19426688922257290709194619068235189066424068390521395212518124097389042852052084981 76}.$$

By computation, we can get $(\frac{3}{1000}, P_2, K_2)$ is the real root of f_2, and $f_3(\frac{3}{1000}, P_2, K_2) < f_3^+(\frac{3}{1000}, \overline{P}_2, \overline{K}_2) + f_3^-(\frac{3}{1000}, \underline{P}_2, \underline{K}_2) \approx -6.710213765 \times 10^{-26}$, which implies that $(\frac{3}{1000}, P_2, K_2)$ is a common zero of $\{f_1, f_2\}$, but not a common zero of $\{f_1, f_2, f_3\}$. Then E_2 is a weak focus of order 3 when $(m,z,q) = (\frac{3}{1000}, P_2, K_2)$. The proof is completed. □

From the above analysis, we have the following theorem.

Theorem 2.6. *Assume that* $(a,s) = (\bar{a},\bar{s})$ *and* $(m,z,q) \in \Omega$, *then* E_2 *is a weak focus of order up to* 4. *Moreover,*
(1) if $(m,z,q) \in W_1$, *then* E_2 *is a weak focus of order* 1;
(2) if $(m,z,q) \in W_2$, *then* E_2 *is a weak focus of order* 2;
(3) if $(m,z,q) \in W_3$, *then* E_2 *is a weak focus of order* 3;
(4) if $(m,z,q) \in W_4$, *then* E_2 *is a weak focus of order* 4.

Theorem 2.7. *Assume* $(a,s) = (\bar{a},\bar{s})$ *holds. Moreover,*
(1) if $(m,z,q) = (\frac{3}{1000}, P_2, K_2)$, E_2 *is a weak focus of orders 3 and system* (2.1) *undergoes a degenerate Hopf bifurcation of codimension* 3 *around* E_2;
(2) if $(m,z,q) = (M_1, Z_2, Q_2)$, E_2 *is a weak focus of order 4 and system* (2.1) *undergoes a degenerate Hopf bifurcation of codimension* 4 *around* E_2.

Proof. From Lemmas 2.4 and 2.5, we obtain that E_2 is a weak focus of order 3 and 4 when $(m,z,q) = (M_1, Z_2, Q_2)$ and $(m,z,q) = (\frac{3}{1000}, P_2, K_2)$, respectively. Using Maple, we have

$$\Phi_1 := \left| \frac{\partial(\mathrm{Tr}(E_2), L_1, L_2)}{\partial(m,z,q)} \right|_{(a,s,m)=(\bar{a},\bar{s},\frac{3}{1000})} = \frac{125 \times 10^{36} z^7 J_1(z,q)}{576 D_0^6 (1000z-3)^5 (z-1)^4},$$

$$\Phi_2 := \left|\frac{\partial(\mathrm{Tr}(E_2), L_1, L_2, L_3)}{\partial(m, z, q, a)}\right|_{(a,s)=(\bar{a},\bar{s})} = -\frac{z^{12}(3qz+s)J_2(m,z,q)}{254803968D_0^{\frac{21}{2}}(m-z)^6(z-1)^6},$$

where $J_1(z,q)$ and $J_2(m,z,q)$ are omitted for brevity. Obviously, the denominator of Φ_1 is nonzero for $m = \frac{3}{1000}$ and $(z,p) \in \Omega_*$. Also, it is easy to obtain all the factors of Φ_2 are nonzero except J_2. Hence, the signs of Φ_1 and Φ_2 are determined by J_1 and J_2, respectively.

Using Theorem 2.2 of [28] again, we have

$$J_1(P_2, K_2) > J^-(\overline{P}_2, \overline{K}_2) + J^+(\underline{P}_2, \underline{K}_2) \approx 9.330545333 \times 10^{-31} > 0,$$
$$J_2(M_1, Z_2, Q_2) < J^+(\overline{M}_1, \overline{Z}_2, \overline{Q}_2) + J^-(\underline{M}_1, \underline{Z}_2, \underline{Q}_2) \approx -3.326028347 \times 10^{-48} < 0.$$

Thus, $\Phi_1 \neq 0$ when $(m,z,q) = \left(\frac{3}{1000}, P_2, K_2\right)$. This implies that system (2.1) undergoes a degenerate Hopf bifurcation of codimension 3 around E_2. Moreover, since $\Phi_2 \neq 0$ when $(m,z,q) = (M_1, Z_2, Q_2)$, system (2.1) exhibits a degenerate Hopf bifurcation of codimension 4 around E_2. The proof is completed. □

2.4. Numerical simulations

The dynamical behavior of system (2.1) is primarily influenced by two key factors: (i) Allee effect, affecting prey population survival at low densities, and (ii) Smith growth, controlling prey population expansion. Numerical simulations give to illustrate the influence of Allee effect and Smith growth on the dynamic behaviors of system (2.1).

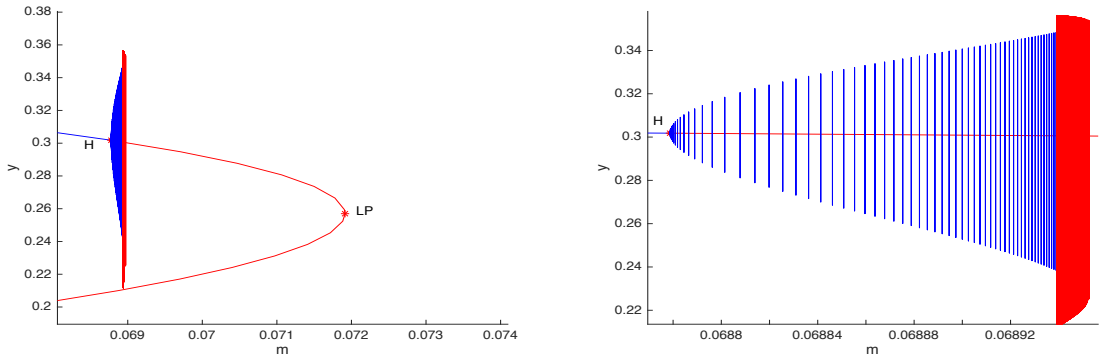

(a) (b)

Figure 6. (a) Bifurcation diagram of system (2.1) in the (m,y) plane with $(a,q,s) = (0.17391, 0.5122, 0.12568)$. (b) Local amplified phase portrait of (a).

2.4.1. The impact of Allee effect

To investigate the influence of the Allee effect, we analyze system (2.1) with fixed parameters $(a,q,s) = (0.17391, 0.5122, 0.12568)$ while varying the Allee threshold m (see Figure 6). Our analysis reveals the following dynamical regimes:

(1) When $m = 0.064$, system (2.1) has two positive equilibria: A saddle point E_1 and a stable focus E_2 (see Figure 7(a)).

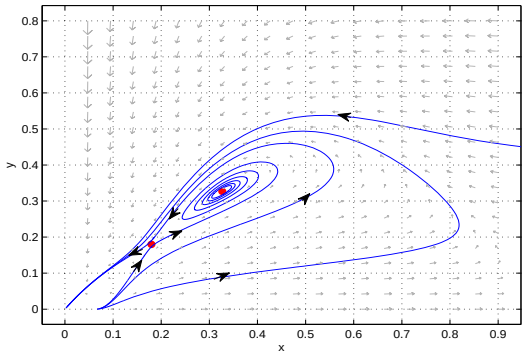

(a) $m = 0.064$

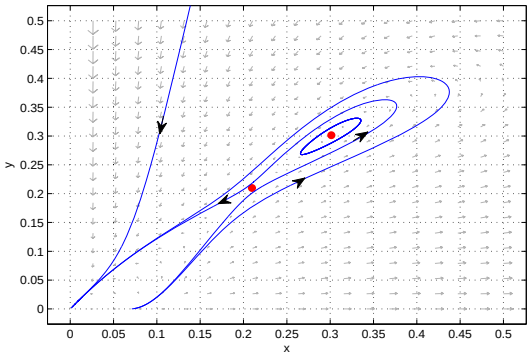

(b) $m = 0.06885$

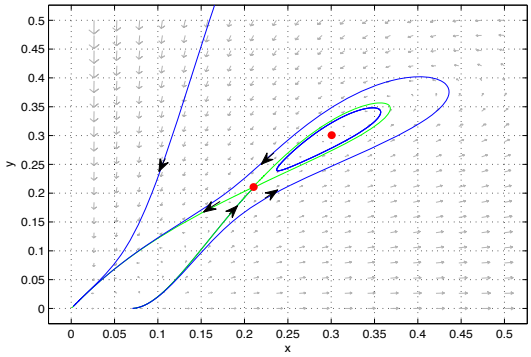

(c) $m = 0.0689391$

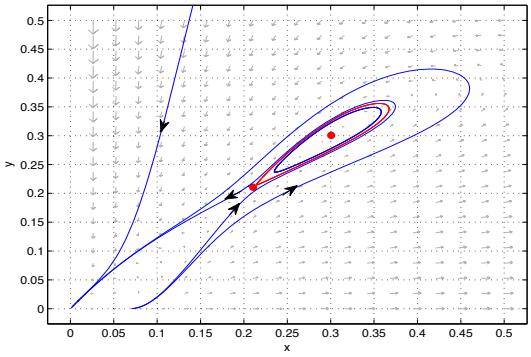

(d) $m = 0.0689434$

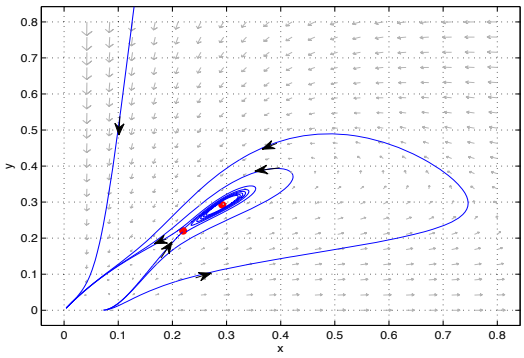

(e) $m = 0.07$

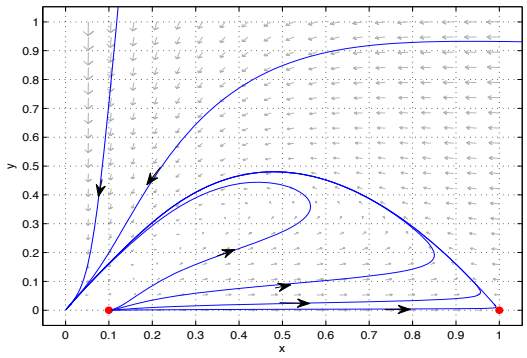

(f) $m = 0.1$

Figure 7. Phase portraits of system (2.1) with $a = 0.17391, q = 0.5122, s = 0.12568$.

(2) When $m = 0.06885$, a supercritical Hopf bifurcation occur at E_2, which will turn the stable focus into an unstable focus and thereby will generate a stable limit cycle.

This indicates that predators and prey can coexist in periodic oscillation (see Figure 7(b)).

(3) When $m = 0.0689391$, system (2.1) has a homoclinic orbit that coexists with an inner stable limit cycle (see Figure 7(c)).

(4) When $m = 0.0689434$, system (2.1) has two limit cycles, where the inner one is stable and the outer is unstable (see Figure 7(d)). Here, the outer limit cycle acts as a separatrix, making the coexistent or extinction of predator and prey are sensitive to the initial conditions.

(5) When $m = 0.07$, system (2.1) undergoes a saddle-node bifurcation of limit cycle, and both two limit cycles disappear (see Figure 7(e)). This leads to the disruption of the coexistence of predator and prey, and also increases the risk of species extinction.

(6) When $m = 0.1$, all positive equilibria vanish (see Figure 7(f)), that is all the trajectories converge towards the origin, implying that the strong Allee effect eliminates the possibility of predator-prey coexistence.

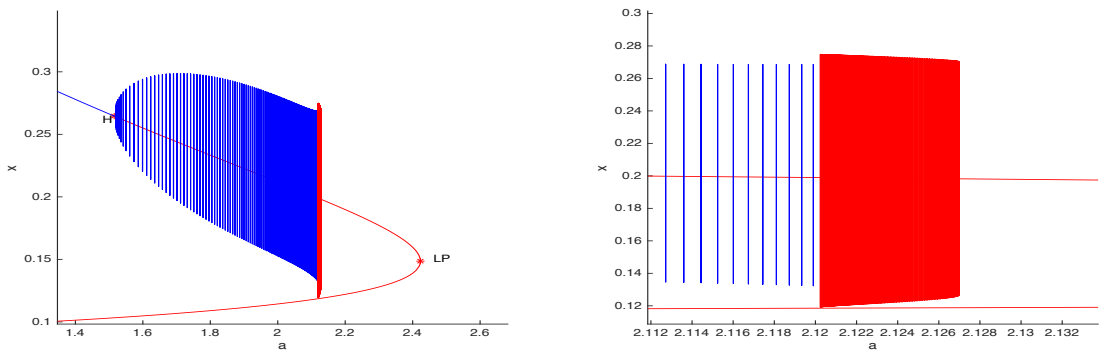

(a) (b)

Figure 8. (a) Bifurcation diagram in the (a, x) plane with $(m, q, s) = (0.04534, 0.435, 0.06455)$, (b) Local amplified phase portrait of (a).

2.4.2. The impact of Smith growth

In order to discuss the influence of the Smith growth on the dynamic behaviors of system (2.1), we let $(m, q, s) = (0.04534, 0.435, 0.06455)$ and draw the bifurcation diagram of the parameter a by Matcont software (see Figure 8).

(1) When the Smith growth parameter $a = 1.4$, system (2.1) admits two positive equilibria: A saddle point E_1 and a stable focus E_2 (see Figure 9(a)). In this case, the stable manifold of a saddle acts as a separatrix, the predator and prey can coexist at a steady state or both become extinct according the initial values.

(2) As a increases to 1.8, E_2 loses its stability through a supercritical Hopf bifurcation and generates a stable limit cycle (see Figure 9(b)), which implies that predator and prey can coexist in periodic oscillation.

(3) When $a = 2.1202$, a homoclinic loop emerges, while a stable limit cycle still surrounds E_2 (see Figure 9(c)), indicating complex dynamics and bistability.

(4) When $a = 2.125$, two limit cycles coexist: An inner stable limit cycle and an outer unstable one (see Figure 9(d)).

(5) When $a = 2.42$, system (2.1) undergoes a saddle-node bifurcation of limit cycle, and two limit cycles disappeared, while system (2.1) still has two equilibria E_1 and E_2.

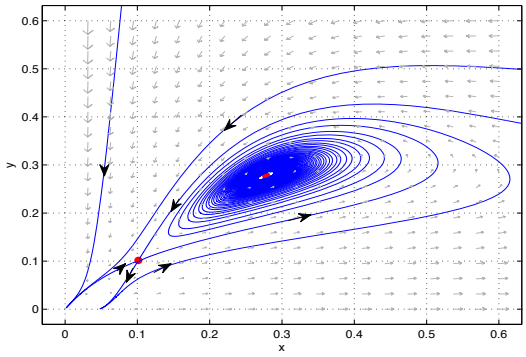

(a) $a = 1.4$

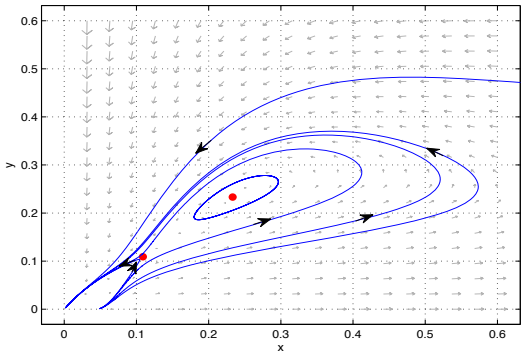

(b) $a = 1.8$

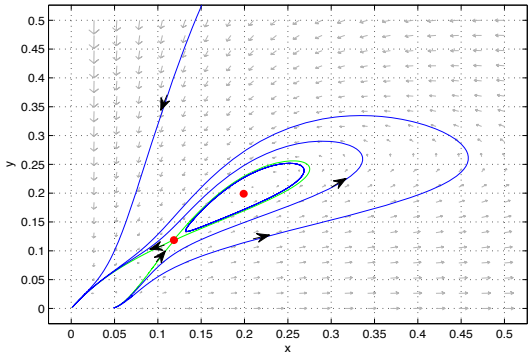

(c) $a = 2.1202$

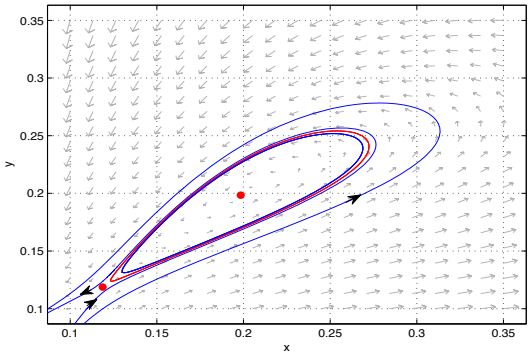

(d) $a = 2.125$

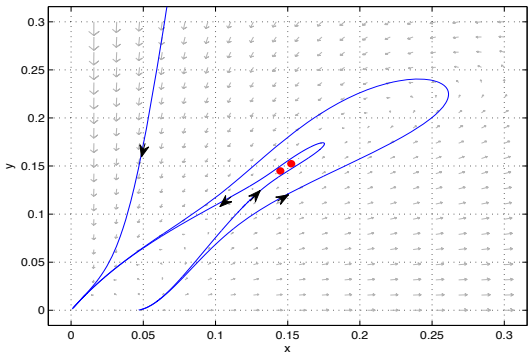

(e) $a = 2.42$

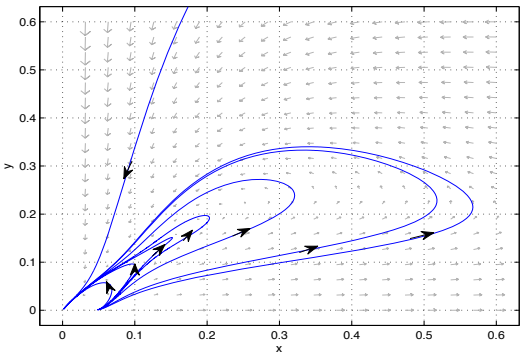

(f) $a = 2.5$

Figure 9. Phase portraits of system (2.1) with $(m, q, s) = (0.04534, 0.435, 0.06455)$.

(6) Finally, when $a = 2.5$, system (2.1) undergoes a saddle-node bifurcation, and admits no positive equilibrium (see Figure 9(f)). This suggests that under high levels of Smith growth,

neither species can persist, leading to eventual extinction.

These observations suggest that excessive Allee effect and Smith growth can lead to the breakdown of species coexistence, and ultimately cause the extinction of prey and predator through a sequence of bifurcations.

3. Changing environment

In real-world ecosystems, environmental conditions are rarely static and often fluctuate over time. As a result, the parameters in predator-prey model, such as resource availability and species carrying capacities, are inherently time-dependent. Ecologists are increasingly interested in understanding how these temporal variations influence the dynamic behaviors of multiple species and whether these changes can give rise to novel ecological behaviors.

Based on the theoretical results of system (1.3) with constant environment ($\mu = 0$) in Section 2, we now investigate the dynamics of system (1.4) with changing environment ($\mu \neq 0$). Here, μ represents the rate of environmental change, influencing the time evolution of the prey's carrying capacity $K(t)$. This section aims to analyze how different values of μ affect the dynamic behaviors of system (1.4).

We employ the numerical simulation method to study the impact of changing environment on system (1.4). First, we utilize the bifurcation analysis software Matcont to construct one-parameter bifurcation diagrams of system (1.3) in the K-x and K-x-y planes (constant environment), respectively.

Next, we simulate trajectories of system (1.4), and project some "representative" trajectories onto the K-x and K-x-y planes to generate representative "time series" that reflect how solutions evolve as $K(t)$ changes dynamically.

In Figures 10-15, the stable and unstable equilibria of system (1.3) are illustrated by black solid and dashed curves, and the maximum and minimum values of stable and unstable oscillations are indicated by blue and black open circles, respectively. In system (1.4), the carrying capacity $K(t)$ increases over time when $\mu > 0$ and decreases when $\mu < 0$. Based on the bifurcation diagrams of system (1.3), we classify the dynamics of system (1.4) into two primary cases according to the sign and magnitude of μ, and systematically analyze each case.

Case (I). Bistability (a stable steady state and a stable oscillation). When system (1.3) undergoes a supercritical Hopf bifurcation around E_2, system (1.3) exhibits bistability (a stable steady state and a stable oscillation) (see Figure 10). In Figures 10(a) and 10(b), where the carrying capacity $K(t)$ increases with time due to $\mu > 0$, we observe that the prey $x(t)$ in system (1.4) (represented by the red and green curve), either tends to the origin (the green curve), or initially tracking the stable equilibrium E_2 of system (1.3), continues along the unstable E_2 as $K(t)$ crosses the Hopf bifurcation point (denoted by H), and eventually converges to a stable oscillation (the red curve). This process illustrates slow environmental change can lead to a regime shift from steady coexistence to persistent stable oscillations by tracking of unstable steady states.

Conversely, in Figures 10(c) and 10(d), where $\mu < 0$, that is $K(t)$ decreases, the prey population either directly tends to the origin (the cyan curve), or may transiently track the stable oscillation before returning to the stable equilibrium E_2, and eventually converges to the origin (see the blue curve). Therefore, when the environmental changes are relatively slow, predator and prey will be a longer transient states before it eventually becomes extinct.

Case (II). Bistability (two stable states). When system (1.3) undergoes a subcritical Hopf bifurcation around $E_2(x_2, y_2)$, system (1.3) may exhibit bistability, with two stable equilibria:

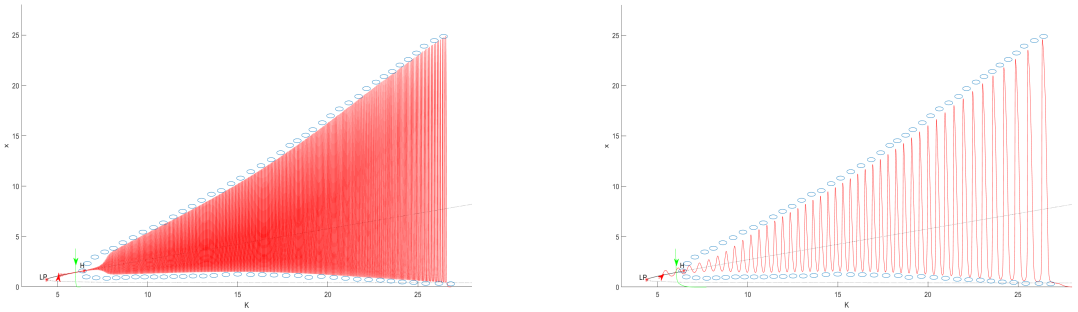

(a) $\mu = 0.005$ (b) $\mu = 0.05$

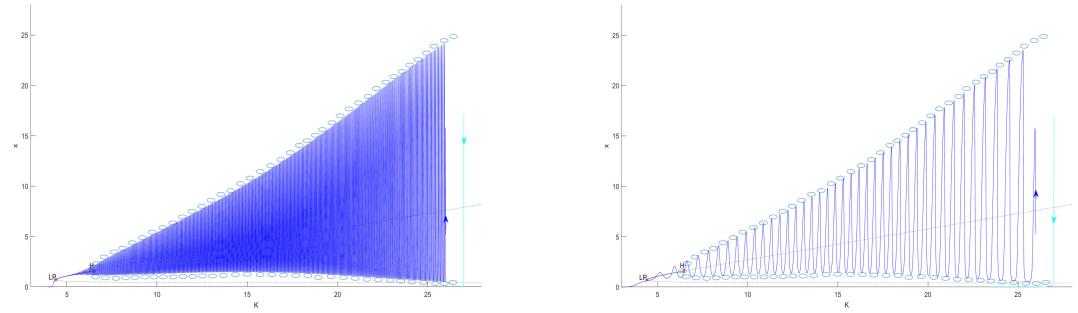

(c) $\mu = -0.005$ (d) $\mu = -0.05$

Figure 10. Dynamics in system (1.4) for different rate of environmental change with $n = 0.5$, $s = 0.525$, $m = 0.225$, $q = 1.3$, $r = 1.5$ and $a = 2$. The initial points of the green, red, blue and cyan curves are $(x(0), y(0), K(0)) = (4, 2, 6)$, $(0.8, 0.4, 5)$, $(5, 2.5, 26)$ and $(18, 9, 27)$, respectively. LP and H represent saddle-node and supercritical Hopf bifurcation, respectively.

E_2 and the extinction state $(0, 0)$ which coexist with an unstable limit cycle (see Figure 11). As shown in Figure 11(a), the prey population $x(t)$ in system (1.4) (red curve) can either tend to extinction or initially track the unstable oscillatory state created by the subcritical Hopf bifurcation, before eventually converging to the positive equilibrium E_2 (the cyan curve). This highlights the role of initial conditions in shaping long-term dynamics such as coexistence or extinction, due to the presence of multiple attractors and bifurcation-induced regime shifts. Moreover, Figures 11(b) and 11(c) demonstrate that under slower environmental change, the prey $x(t)$ remains close to the coexistence state E_2 for a longer duration before ultimately collapsing to extinction. These results suggest that ecological systems near critical transitions can exhibit transient tracking behavior, where populations temporarily tracking unstable states before eventually shifting to a new stable regime. The rate of environmental change significantly influences the persistence time and the eventual ecological dynamics.

Delay or avoid extinction. Figures 16 and 17 illustrate the coexistence and extinction of predator and prey with changing environment. In Figure 16(a), for $\mu > 0$ and initial conditions close to the stable state, we observe three types of dynamical behaviors.

For small $|\mu|$, the green trajectory quickly collapses to extinction. As $|\mu|$ gradually increases, the red trajectory temporarily can track the unstable steady state before extinction. When $|\mu|$ is large enough, the magenta trajectory tracks the unstable steady state, and then switches to

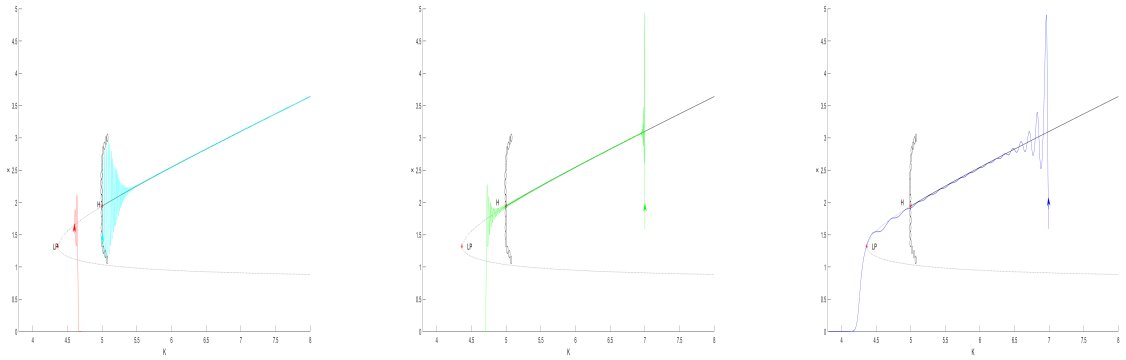

(a) $\mu = 0.0005$ (b) $\mu = -0.0005$ (c) $\mu = -0.005$

Figure 11. Dynamics of system (1.4) for different rates of environmental change with $n = 1$, $s = 0.176133$, $m = 0.5$, $q = 0.18$, $r = 0.5$ and $a = 0.67211$. The initial points of the red and cyan curves are $(x(0), y(0), K(0)) = (1.5, 1.5, 4.6)$, $(1.5, 1.5, 5)$, and the initial points of the green and blue curves is $(x(0), y(0), K(0)) = (1.5, 1.5, 7)$. LP and H represent saddle-node and subcritical Hopf bifurcation, respectively.

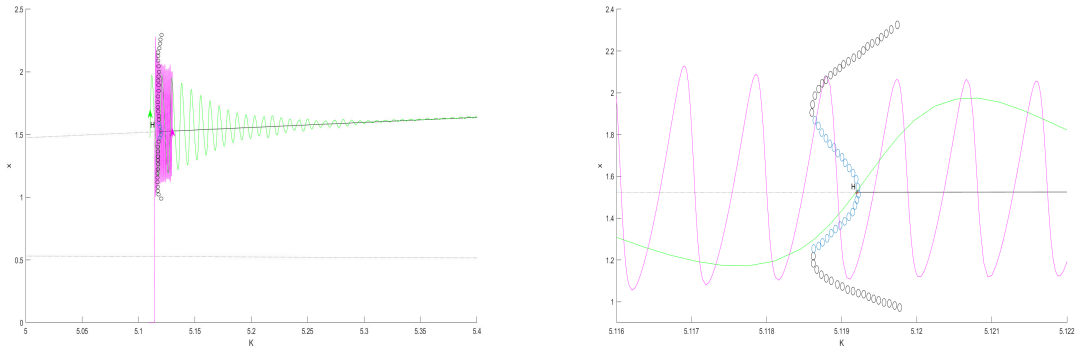

(a) (b)

Figure 12. Dynamics of system (1.4) for different rate of environmental change μ: The green curve represents $\mu = 0.00005$ and the red curve represents $\mu = -0.000005$ with $n = 1$, $s = 0.0016$, $m = 0.4$, $q = 0.0268$, $r = 0.483$ and $a = 28$. LP and H represent saddle-node and supercritical Hopf bifurcation, respectively. (b) is the local amplified phase portrait of (a).

stable oscillation before ultimately collapsing to extinction. In Figure 16(b), for $\mu < 0$ and initial conditions far from the stable state, a similar phenomenon of delay extinction is observed. Hence, when the change of changing environment is fast (that is $|\mu|$ is large), then the prey and predator can delay extinct, that is the rapidly changing environment is conducive to the survival of prey and predator.

In Figure 17(a), considering $\mu > 0$, initial conditions are not close to the stable state. For small μ, the solutions (the green curve) first track the unstable oscillation and then tend to track the stable state; thus the populations avoid extinction. For large μ, the time for the solution (the magenta curve) to reach a unstable oscillation is rather short. That is the solutions will first track the oscillation with a small amplitude, and ultimately switch to the stable state. It reveals that slow positive environmental change can enable the system to reach a new stable state more

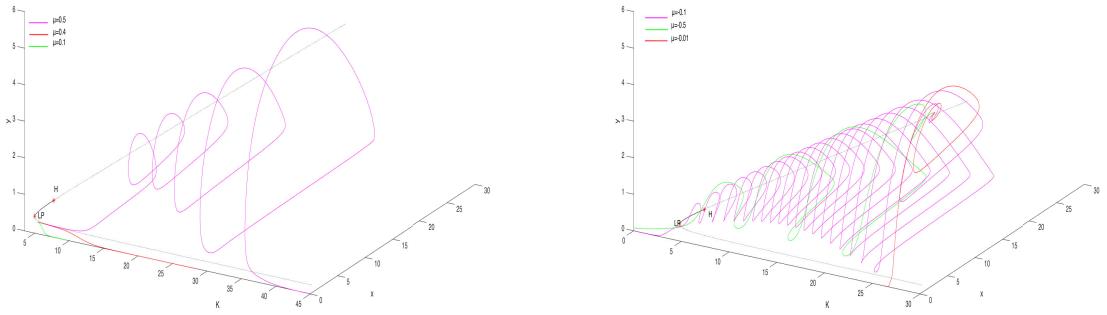

(a) (b)

Figure 13. Dynamics of system (1.4) in K-x-y space for different μ with with $n = 0.5$, $s = 0.525$, $m = 0.225$, $q = 1.3$, $r = 1.5$ and $a = 2$. (a) $(x(0), y(0), K(0)) = (0.5, 0.25, 4.9)$, (b) $(x(0), y(0), K(0)) = (8, 4, 27)$.

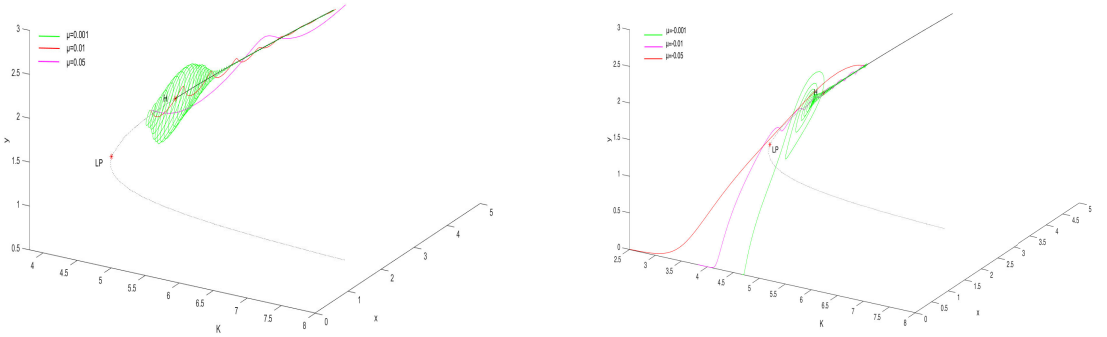

(a) (b)

Figure 14. Dynamics of system (1.4) in K-x-y space for different μ with $n = 1$, $s = 0.176133$, $m = 0.5$, $q = 0.18$, $r = 0.5$ and $a = 0.67211$. (a) $(x(0), y(0), K(0)) = (1.8, 1.8, 4.7)$, (b) $(x(0), y(0), K(0)) = (2.3, 2.3, 5.6)$.

quickly (fast regime shift). In contrast, Figure 17(b), with $\mu < 0$ and initial conditions near the stable state, shows that fast environmental deterioration (large $|\mu|$, red trajectory) causes extinction after passing the saddle-node (LP), whereas slower change (green trajectory) leads to extinction after the Hopf point (H). These observations suggest that fast negative environmental change can delay extinction, while slow positive change can prevent it.

Under certain parameter values, system (1.3) can exhibit rich dynamics, that is it may simultaneously exist a stable extinction state $(0, 0)$, an unstable or stable equilibrium E_2, and two limit cycles (the inner one is stable and the outer one is unstable), see Figure 15. In such cases, the corresponding system (1.4) can display complex transient behaviors driven by changing environment. For instance, in Figure 15(a), the green trajectory initially follows the stable oscillation when it crosses a Hopf bifurcation point (H), and eventually converges to the stable

positive equilibrium E_2. In contrast, the magenta trajectory initially attracted by the stable oscillation, ultimately collapses to extinction. These phenomena reflect even minor changes in initial conditions or environmental parameters can cause sudden shifts in species between qualitatively different long-term dynamics.

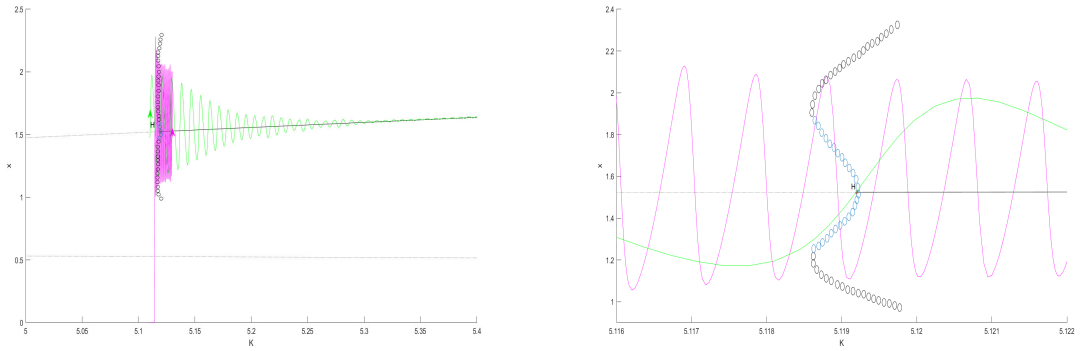

(a) (b)

Figure 15. Dynamics of system (1.4) for different rate of environmental change μ: The green curve represents $\mu = 0.00005$ and the red curve represents $\mu = -0.000005$ with $n = 1$, $s = 0.0016$, $m = 0.4$, $q = 0.0268$, $r = 0.483$ and $a = 28$. LP and H represent saddle-node and supercritical Hopf bifurcation, respectively. (b) is the local amplified phase portrait of (a).

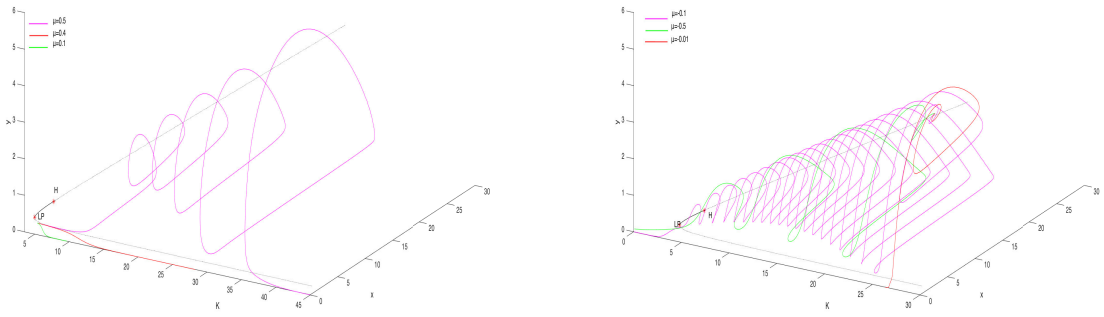

(a) (b)

Figure 16. Dynamics of system (1.4) in K-x-y space for different μ with with $n = 0.5$, $s = 0.525$, $m = 0.225$, $q = 1.3$, $r = 1.5$ and $a = 2$. (a) $(x(0), y(0), K(0)) = (0.5, 0.25, 4.9)$, (b) $(x(0), y(0), K(0)) = (8, 4, 27)$.

4. Conclusion

In this paper, considering constant environment and changing environment, we study the bifurcation and transient dynamics of a Leslie-Gower predator-prey model incorporating Smith growth function and Allee effect.

For constant environment, that is system (1.3), we show that the two boundary equilibria are unstable. Furthermore, we rigorously proved that the origin is an attractor, providing a

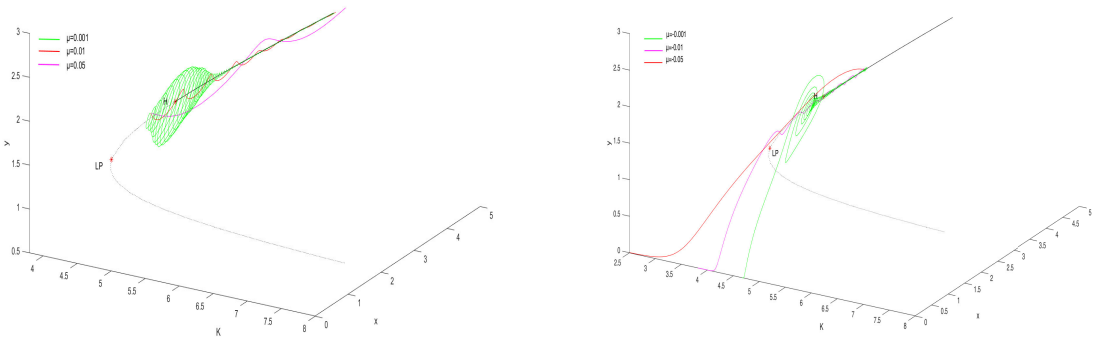

(a) (b)

Figure 17. Dynamics of system (1.4) in K-x-y space for different μ with $n = 1$, $s = 0.176133$, $m = 0.5$, $q = 0.18$, $r = 0.5$ and $a = 0.67211$. (a) $(x(0), y(0), K(0)) = (1.8, 1.8, 4.7)$, (b) $(x(0), y(0), K(0)) = (2.3, 2.3, 5.6)$.

foundation for understanding extinction scenarios in this system. Compared with earlier work on the model without Smith growth [30, 39], which identified degenerate Bogdanov–Takens bifurcations of codimension three and degenerate Hopf bifurcations of codimension two, the present study shows that incorporating Smith growth and the Allee effect markedly enhances the dynamical complexity of the system, resulting in bifurcations of higher codimension, such as degenerate Hopf bifurcations of codimension four.

In contrast, our results indicate that the introduction of Smith growth and Allee effect has greatly enriched the dynamics of the system and led to more complex bifurcation with higher codimension. More precisely, we showed that system (1.3) has a cusp of codimension three and undergoes a saddle-node bifurcation and degenerate Bogdanov-Takens bifurcation of codimension three. In particular, using the real root isolation algorithm of multivariate polynomial system, we have rigorously proved that the positive equilibrium of system (1.3) is a weak focus of order four and system (1.3) exhibits a degenerate Hopf bifurcation of codimension four.

Also, our results offer significant ecological insights. The Smith growth function influences not only the prey population (to which it is directly applied) but also indirectly affects predator dynamics. When the Smith growth parameter lies within a suitable range, both predator and prey will coexist stably. However, if this parameter becomes large, it can lead to the extinction of both species, demonstrating that excessive Smith growth can be detrimental to community stability. Furthermore, we find that the Allee effect plays a crucial role in the survival of species. That is, the weaker Allee effect is conducive to the stable coexistence of species, while the stronger Allee effect disrupts the balance among species and eventually leads to species extinction.

For changing environment, incorporating a time-dependent carrying capacity into system (1.3) to reflect continuous environmental change, we investigated how the rate of changing environment influences transient dynamics of system (1.4). By comparing these transient dynamics with the bifurcation structure of the corresponding constant environment system (1.3), we found that rich transient dynamics, such as tracking of unstable equilibria or limit cycles, delay or avoid extinction, and slow and fast regime shifts. We showed that ecological systems near critical transitions can exhibit transient tracking behavior, where populations temporarily tracking unstable states before eventually shifting to a new stable regime. In some situation, fast negative environmental

change can delay extinction, while slow positive change can prevent it. These results highlight the significance of transient dynamics in ecology and demonstrate that incorporating changing environment into ecological models can reveal potential risks to species persistence.

Finally, several directions for future research naturally emerge from the present work. One possible extension is to incorporate other functional response functions, which may further enrich the dynamical behavior of the system. Another important direction is to consider predator populations with additional food sources, which could significantly alter persistence conditions and bifurcation structures. Such extensions may provide a more comprehensive understanding of complex ecological interactions in realistic environments.

In summary, the combined effects of Smith growth and Allee effect not only enriches the dynamical complexity of systems (1.3) and (1.4) but also gives rise to a series of transient dynamics and high-dimensional bifurcation phenomena, including degenerate Bogdanov-Takens of codimension 3 and degenerate Hopf bifurcations of codimension four. These results demonstrate the importance of incorporating biologically realistic mechanisms in ecological modeling to better understand complex species interactions.

Acknowledgement

This work was supported by the Scientific Research Foundation of Minjiang University (MJY22027) and Natural Science Foundation of Fujian Province (2025J01488, 2025J011265).

References

[1] W. C. Allee, *Animal aggregations*, The Quarterly Review of Biology, 1927, 2, 367–398.

[2] R. Arumugam, F. Guichard and F. Lutscher, *Persistence and extinction dynamics driven by the rate of environmental change in a predator–prey metacommunity*, Theoretical Ecology, 2020, 13, 629–643.

[3] R. Arumugam, F. Lutscher and F. Guichard, *Tracking unstable states: Ecosystem dynamics in a changing world*, Oikos, 2021, 130, 525–540.

[4] D. Bai, J. Zheng and Y. Kang, *Global dynamics of a predator–prey model with a Smith growth function and additive predation in prey*, Discrete and Continuous Dynamical Systems–B, 2024, 29, 1923–1960.

[5] J. Cao, L. Ma and P. Hao, *Bifurcation analysis in a modified Leslie–Gower predator–prey model with Beddington–DeAngelis functional response*, Journal of Applied Analysis & Computation, 2023, 13, 3026–3053.

[6] Q. Cao, X. Bao and X. Yi, *Dynamics of a predator–prey model with Allee effect and herd behavior*, Journal of Nonlinear Modeling and Analysis, 2024, 6, 392–412.

[7] X. Chen and W. Yang, *Complex dynamical behaviors of a Leslie–Gower predator–prey model with herd behavior*, Journal of Nonlinear Modeling and Analysis, 2024, 6, 1064–1082.

[8] X. Chen and W. Zhang, *Decomposition of algebraic sets and applications to weak centers of cubic systems*, Journal of Computational and Applied Mathematics, 2009, 232, 565–581.

[9] F. Dumortier, R. Roussarie and J. Sotomayor, *Generic 3-parameter families of vector fields on the plane, unfolding a singularity with nilpotent linear part. The cusp case of codimension three*, Ergodic Theory and Dynamical Systems, 1987, 7, 375–413.

[10] X. Feng, X. Liu, C. Sun and Y. Jiang, *Stability and Hopf bifurcation of a modified Leslie–Gower predator–prey model with Smith growth rate and Beddington–DeAngelis functional response*, Chaos, Solitons & Fractals, 2023, 174, 113794.

[11] X. Fu and H. Jiang, *Turing–Hopf bifurcation in a diffusive predator–prey model with schooling behavior and Smith growth*, Applied Mathematics Letters, 2025, 159, 109257.

[12] M. He and Z. Li, *Global dynamics of a Leslie–Gower predator–prey model with square root response function*, Applied Mathematics Letters, 2023, 140, 108561.

[13] J. Huang, Y. Gong and J. Chen, *Multiple bifurcations in a predator–prey system of Holling and Leslie type with constant-yield prey harvesting*, International Journal of Bifurcation and Chaos, 2013, 23, 1350164.

[14] J. Huang, Y. Gong and S. Ruan, *Bifurcation analysis in a predator–prey model with constant-yield predator harvesting*, Discrete and Continuous Dynamical Systems–B, 2013, 18(8), 2101–2121.

[15] J. Huang, M. Lu, C. Xiang and L. Zou, *Bifurcations of codimension four in a Leslie-type predator–prey model with Allee effects*, Journal of Differential Equations, 2025, 414, 201–241.

[16] J. Huang, S. Ruan and J. Song, *Bifurcations in a predator–prey system of Leslie type with generalized Holling type III functional response*, Journal of Differential Equations, 2014, 257(6), 1721–1752.

[17] N. Martinez-Jeraldo and A. Pablo, *Allee effect acting on the prey species in a Leslie–Gower predation model*, Nonlinear Analysis: Real World Applications, 2019, 45, 895–917.

[18] A. Korobeinikov, *A Lyapunov function for Leslie–Gower predator–prey models*, Applied Mathematics Letters, 2001, 14, 697–699.

[19] V. Kumar, *Pattern formation and delay-induced instability in a Leslie–Gower type prey–predator system with Smith growth function*, Mathematics and Computers in Simulation, 2024, 225, 78–97.

[20] P. H. Leslie, *Some further notes on the use of matrices in population mathematics*, Biometrika, 1948, 35, 213–245.

[21] P. H. Leslie, *A stochastic model for studying the properties of certain biological systems by numerical methods*, Biometrika, 1958, 45, 16–31.

[22] S. Li, S. Yuan, Z. Jin and H. Wang, *Bifurcation analysis in a diffusive predator–prey model with spatial memory of prey, Allee effect and maturation delay of predator*, Journal of Differential Equations, 2023, 357, 32–63.

[23] Y. Li, M. He and Z. Li, *Dynamics of a ratio-dependent Leslie–Gower predator–prey model with Allee effect and fear effect*, Mathematics and Computers in Simulation, 2022, 201, 417–439.

[24] Z. Li and M. He, *Hopf bifurcation in a delayed food-limited model with feedback control*, Nonlinear Dynamics, 2014, 76, 1215–1224.

[25] Y. Liu, Z. Zhang and Z. Li, *The impact of Allee effect on a Leslie–Gower predator–prey model with hunting cooperation*, Qualitative Theory of Dynamical Systems, 2024, 23, 88.

[26] M. Lu, J. Huang and H. Wang, *An organizing center of codimension four in a predator–prey model with generalist predator: From tristability and quadristability to transients in a*

nonlinear environmental change, SIAM Journal on Applied Dynamical Systems, 2023, 22, 694–729.

[27] M. Lu, C. Xiang, J. Huang and S. Ruan, *Dynamics of the generalized Rosenzweig–MacArthur model in a changing and patchy environment*, Physica D: Nonlinear Phenomena, 2024, 465, 134197.

[28] Z. Lu, B. He, Y. Lou and L. Pan, *An algorithm of real root isolation for polynomial systems with application to the construction of limit cycles*, Symbolic–Numeric Computation, 2007, 232, 131–147.

[29] Y. Ma and R. Yang, *Bifurcation analysis in a modified Leslie–Gower model with nonlocal competition and Beddington–DeAngelis functional response*, Journal of Applied Analysis & Computation, 2025, 15, 2152–2184.

[30] E. González-Olivares, J. Mena-Lorca, A. Rojas-Palma and J. D. Flores, *Dynamical complexities in the Leslie–Gower predator–prey model as consequences of the Allee effect on prey*, Applied Mathematical Modelling, 2011, 35, 366–381.

[31] D. Pal, D. Kesh and D. Mukherjee, *Pattern dynamics in a predator–prey model with Smith growth function and prey refuge in predator poisoned environment*, Chinese Journal of Physics, 2024, 92, 366–386.

[32] P. J. Pallav and K. M. Prashanta, *Bifurcation analysis of a modified Leslie–Gower predator–prey model with Beddington–DeAngelis functional response and strong Allee effect*, Mathematics and Computers in Simulation, 2014, 97, 123–146.

[33] L. Perko, *Differential Equations and Dynamical Systems*, Springer, New York, 1996.

[34] F. E. Smith, *Population dynamics in Daphnia magna and a new model for population growth*, Ecology, 1963, 44, 651–663.

[35] Y. Tian and Y. Pei, *An explicit recursive formula for computing the normal forms associated with semisimple cases*, Communications in Nonlinear Science and Numerical Simulation, 2014, 19, 2294–2308.

[36] Y. Tian and Y. Pei, *An explicit recursive formula for computing the normal form and center manifold of general n-dimensional differential systems associated with Hopf bifurcation*, International Journal of Bifurcation and Chaos, 2013, 23, 1350104.

[37] H. Wu, Z. Li and M. He, *Bifurcation analysis of a Holling–Tanner model with generalist predator and constant-yield harvesting*, International Journal of Bifurcation and Chaos, 2024, 34, 2450076.

[38] C. Xiang, J. Huang and H. Wang, *Linking bifurcation analysis of Holling–Tanner model with generalist predator to a changing environment*, Studies in Applied Mathematics, 2022, 149, 124–163.

[39] W. Yin, Z. Li, F. Chen and X. He, *Modeling Allee effect in the Leslie–Gower predator–prey system incorporating a prey refuge*, International Journal of Bifurcation and Chaos, 2022, 32, 2250086.

[40] M. Zhang, Z. Li, F. Chen and L. Chen, *Bifurcation analysis of a Leslie–Gower predator–prey model with Allee effect on predator and simplified Holling type IV functional response*, Qualitative Theory of Dynamical Systems, 2025, 24, 131.

[41] Z. Zhang, T. Ding, W. Huang and Z. Dong, *Qualitative Theory of Differential Equations*, American Mathematical Society, 1992.

Received September 2025; Accepted January 2026; Available online February 2026.